Geophysical, geochemical and geochronological constraints on the geology and mineral potential of the Livingstone Creek area, south-central Yukon (NTS 105E/8)

M. Colpron*
Yukon Geological Survey

S. Carr
Ottawa-Carleton Geoscience Centre, Carleton University, Ottawa, ON

D. Hildes
Aurora Geosciences, Whitehorse, YT

S. Piercey
Department of Earth Sciences, Memorial University of Newfoundland, St. John's, NL

Colpron, M., Carr, S., Hildes, D. and Piercey, S., 2017. Geophysical, geochemical and geochronological constraints on the geology and mineral potential of the Livingstone Creek area, south-central Yukon (NTS 105E/8). *In:* Yukon Exploration and Geology 2016, K.E. MacFarlane and L.H. Weston (eds.), Yukon Geological Survey, p. 47-86.

ABSTRACT

The Livingstone Creek area, known for its coarse placer gold, is underlain by mid-Paleozoic metasedimentary, metavolcanic and metaplutonic rocks of the Yukon-Tanana terrane. These rocks were penetratively deformed, metamorphosed under high-pressure conditions in the Permian, and retrogressed to amphibolite facies before the Early Jurassic. A new VTEM™ Plus, helicopter-borne geophysical survey over the area has helped to enhance the interpretation of the bedrock geology and to identify potential exploration targets. The lithological, geochemical and isotopic characteristics of metavolcanic rocks, as well as Early Mississippian U-Pb dates from two metagranitoid plutons in the Livingstone Creek area are consistent with the regional character of correlative assemblages in the Yukon-Tanana terrane. Mid Permian and Middle Triassic U-Pb dates from two granitic intrusions further constrain the timing of development of transposition foliation in the area. Magnetic anomalies and electromagnetic conductors define potential exploration targets for the source of placer gold in the centre of the Livingstone Creek area. Identification of north-northeast lineaments in the magnetic and electromagnetic data may help to locate late brittle faults that are locally observed, and appear to correspond with enrichment in gold in quartz-carbonate veins. In the eastern part of the study area, coincident magnetic highs and electromagnetic conductors are associated with a greenstone-hosted Cu-Zn anomaly and Ag-Pb vein occurrence. The magnetic intensity data may also be helpful in assisting exploration for magnetite-rich placer deposits.

* maurice.colpron@gov.yk.ca

INTRODUCTION

The Livingstone Creek area, located ~80 km northeast of Whitehorse (Fig. 1), has been the site of intermittent placer gold mining since its discovery around the time of the 1898 Gold Rush (Bostock and Lees, 1938; Bostock, 1957; Levson, 1992). Extensive mining took place from 1898 to the late 1930s when a small settlement including a store, hotel, post office and jail existed at the base of Livingstone Creek. The area is accessible by air to a good airstrip, and via winter road from Whitehorse. It is estimated that >50,000 ounces of gold was extracted from at least seven creeks in the district. The Livingstone Creek district is known for producing coarse nuggets, occasionally cobble sized! Despite the coarse nature of the gold, the district has received only limited hardrock exploration efforts to date.

The area was first mapped at a reconnaissance scale (1:250 000) by Bostock and Lees (1938) and Tempelman-Kluit (1984; 2009). Subsequent studies focused primarily on the structural evolution of the area and provided preliminary geochronological constraints (Hansen, 1989; Hansen *et al.*, 1989; 1991; Harvey *et al.*, 1996; 1997; Gallagher *et al.*, 1998; Gallagher, 1999; Mercier, 2011). In 2004 and 2005, the Yukon Geological Survey (YGS) conducted a detailed bedrock mapping program of the Livingstone Creek area (NTS 105E/8) that established the

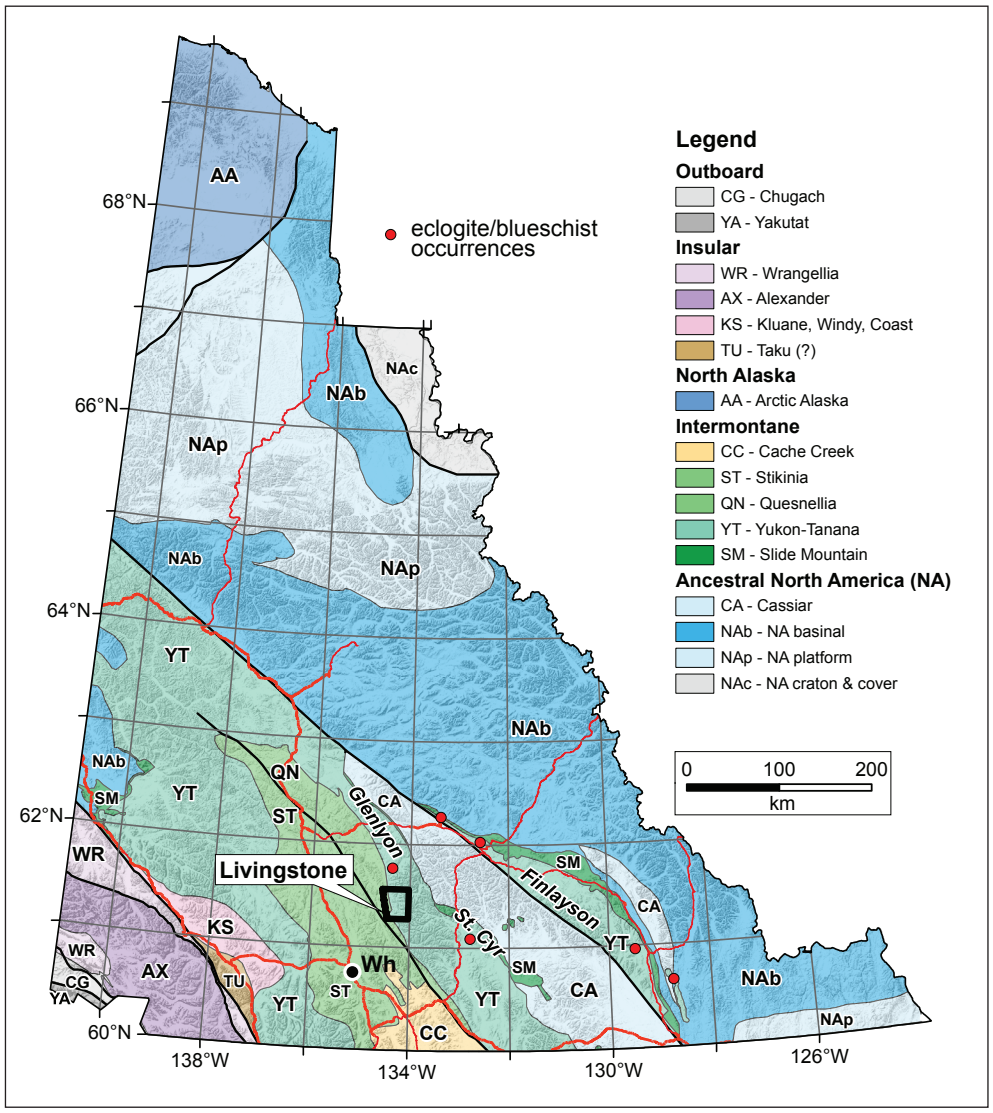

Figure 1. *Terrane map of Yukon illustrating location of the Livingstone Creek area (after Colpron and Nelson, 2011). The Glenlyon, Finlayson and St. Cyr areas, discussed in the text are also indicated, as are occurrences of eclogite and blueschist in the Yukon-Tanana terrane (after Erdmer et al., 1998). Wh = Whitehorse.*

lithological and structural framework of Yukon-Tanana terrane in the area (Colpron, 2005a,b). Although these studies provided preliminary descriptions of map units, supporting geochemical, isotopic and geochronological data remain unpublished.

In 2016, YGS contracted Geotech Ltd. to fly an airborne VTEM™ Plus geophysical survey over the area to further refine the structural framework and help define exploration targets (Boulanger *et al.*, 2016a,b). In this paper we review the geology of the Livingstone Creek area, focusing on the Yukon-Tanana terrane, and highlight some of the results of the VTEM™ Plus survey. We use the geophysical data to develop an enhanced interpretation of the bedrock geology (Colpron, 2017), and also present geochemical, isotopic and geochronological data that constrain the mapped geology. Together these data help develop some observations that shed light on the hardrock and placer potential of the Livingstone Creek area.

REVIEW OF BEDROCK GEOLOGY

The Livingstone Creek area is underlain primarily by mid-Paleozoic metamorphic rocks of the Yukon-Tanana terrane, in the central and eastern part of the area, and by unmetamorphosed mid-Paleozoic to early Mesozoic volcanic and sedimentary rocks of Quesnellia to the southwest (Figs. 1 and 2). Yukon-Tanana and Quesnellia terranes are juxtaposed along the Big Salmon fault zone. To the east, the Yukon-Tanana terrane is dissected by the north-striking d'Abbadie fault (Fig. 2). We present a brief review of the geology of the Yukon-Tanana terrane, following descriptions of Colpron (2005a,b). Rocks of Quesnellia are described by Simard (2003) and Simard and Devine (2003).

The Yukon-Tanana terrane comprises highly strained and transposed metasedimentary, metavolcanic and metaplutonic rocks metamorphosed to upper greenschist and amphibolite facies conditions (Hansen, 1992). High-pressure eclogite metamorphism is locally documented to the north and south of the Livingstone Creek area (Fig. 1; Creaser *et al.*, 1997; Erdmer *et al.*, 1998; Petrie *et al.*, 2016). In the Livingstone Creek area, the terrane can be subdivided into five distinct successions: the Snowcap, Livingstone Creek, Mendocina, Last Peak and Klinkit successions (Fig. 2; Colpron, 2005a; 2017). The first four successions occur mainly in a series of northwest-trending belts. The Klinkit succession is limited to higher elevations and structural levels in the east-central part of the study area.

The **Snowcap assemblage**, exposed in the central part of the map area, comprises quartzite, micaceous quartzite, psammitic schist, carbonaceous phyllite, calcareous chloritic schist, and local exposures of garnet amphibolite and marble (Fig. 2; Colpron, 2005a,b; 2017). Snowcap rocks in the Livingstone Creek area are characteristic of the regional tectonic assemblage as defined in the Glenlyon area to the north (Fig. 1; Colpron *et al.*, 2006; Piercey and Colpron, 2009). The Snowcap assemblage was intruded by the largest Mississippian pluton in the area, which is composed of strongly foliated to gneissic metagranite and metagranodiorite assigned to the **Simpson Range plutonic suite** (Fig. 2; Mortensen, 1992; Colpron *et al.*, 2016a,b). The intrusive sheet and encasing metasedimentary rocks of the Snowcap assemblage form a moderately to steeply southwest-dipping structural panel, and carbonaceous phyllite, chloritic schist and marble are more abundant in the upper structural level to the southwest. Similar rocks of pelitic and psammitic compositions, intruded by Mississippian metaplutonic rocks, also occur in the northeasternmost corner of the Livingstone Creek area, east of d'Abbadie fault (Fig. 2; the Scurvy Creek succession of Westberg, 2009; Westberg *et al.*, 2009).

The **Livingstone Creek succession** comprises mainly light green to light grey quartzite, quartz-muscovite-plagioclase-chlorite schist and greenstone exposed at the headwater of Livingstone and May creeks (Fig. 2; Harvey *et al.*, 1997; Colpron, 2005a,b). Textures in these rocks locally suggest a volcaniclastic origin and they are inferred to be part of the Lower Mississippian Finlayson arc assemblage (Colpron, 2005b; Colpron *et al.*, 2006).

Greenstone (Fig. 3), metagabbro and serpentinite of the **Mendocina succession** form a distinct, ~3 km-wide, northwest-trending belt extending from the headwaters of Livingstone Creek to the northern edge of the map area (Fig. 2; Harvey *et al.*, 1997; Colpron, 2005a,b; 2017), and beyond, to the Big Salmon River to the north (Fig. 4; de Keijzer, 2000; Colpron *et al.*, 2016b). The largest ultramafic body forms a massif at the headwaters of Livingstone (Fig. 5) and May creeks where it is locally altered to nephrite jade (J. Coates, pers. comm., 2016). Magnetite is a common accessory mineral in the serpentinite. Minor occurrences of marble (DMFc) and graphitic phyllite are locally found in the Mendocina greenstone north of Livingstone Creek. The presence of graphitic phyllite may indicate a depositional link with adjacent rocks of the Last Peak succession.

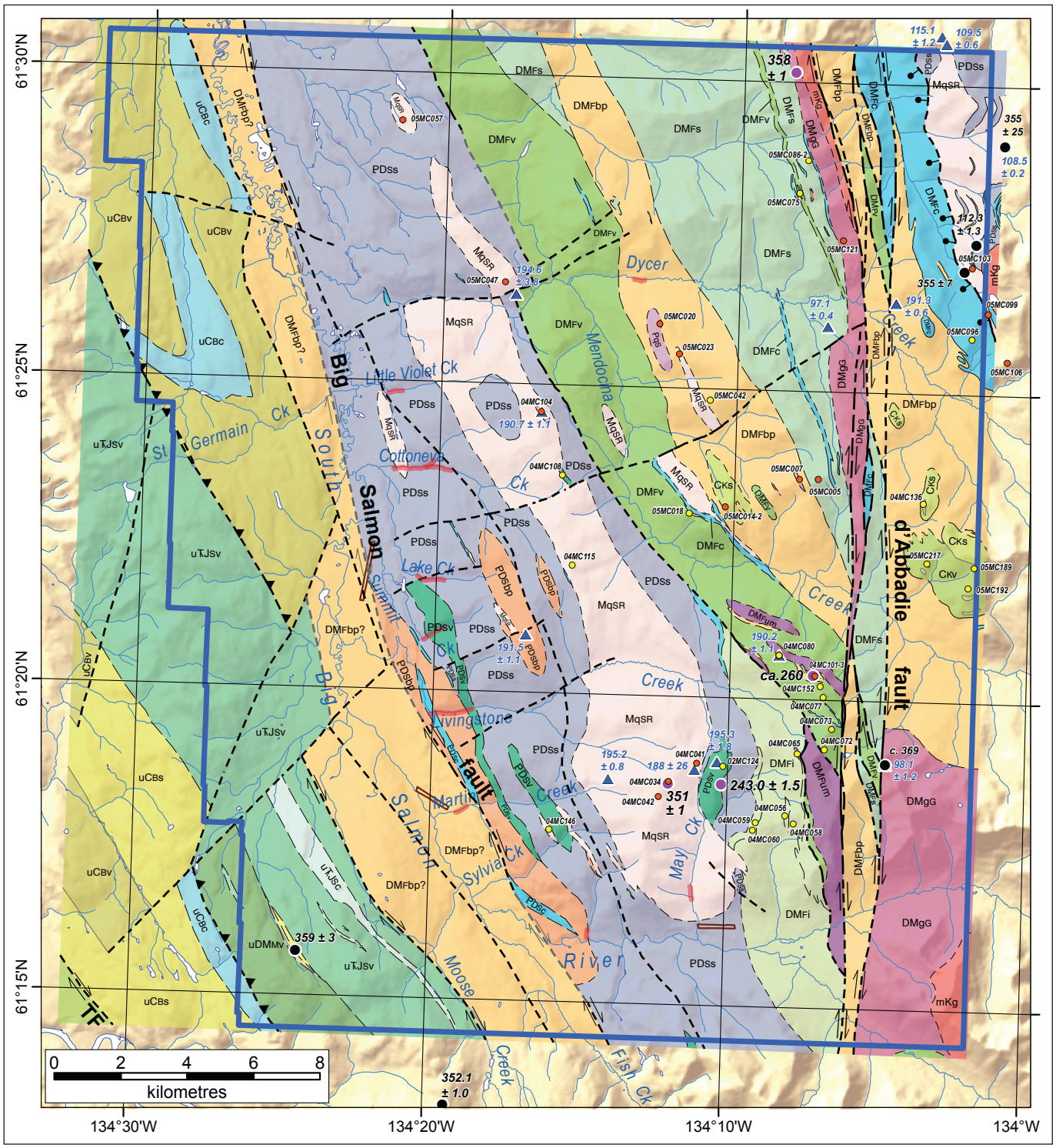

Figure 2. *Simplified geological map of the Livingstone Creek area (after Colpron, 2017). Area covered by VTEM™ Plus survey indicated by heavy blue outline. TF = Teslin fault. Accompanying legend on next page.*

MID-CRETACEOUS

mKg granodiorite, granite

QUESNELLIA

UPPER TRIASSIC TO LOWER JURASSIC

SEMENOF FORMATION

uTJSc limestone

uTJSv basalt, andesite

UPPER CARBONIFEROUS

BOSWELL FORMATION

uCBs slate, phyllite, greywacke, chert

uCBv altered basalt, volcanic breccia

uCBc limestone

UPPER DEVONIAN TO MISSISSIPPIAN

MOOSE FORMATION

uDMv basalt, greenstone

YUKON-TANANA TERRANE

Klondike assemblage

MIDDLE PERMIAN

SULPHUR CREEK SUITE?

PqS foliated two-mica granite

Klinkit assemblage

CARBONIFEROUS

CKv intermediate to mafic metavolcanic rocks

CKs metaclastic rocks, conglomerate

Finlayson assemblage

DEVONIAN TO MISSISSIPPIAN

LAST PEAK SUCCESSION

DMFs siliciclastic and metavolcaniclastic rocks, minor greenstone

DMFbp carbonaceous phyllite, quartzite, chert

DMFc carbonate, marble

MENDOCINA SUCCESSION

DMFum serpentinite, metagabbro

DMFv mafic metavolcanic rocks

LIVINGSTONE CREEK SUCCESSION

DMFi intermediate metavolcaniclastic and siliciclastic rocks

MISSISSIPPIAN

SIMPSON RANGE SUITE

MqSR foliated to gneissic granite, granodiorite

LATE DEVONIAN TO MISSISSIPPIAN

GRASS LAKES SUITE ?

DMgG augen granite

Snowcap assemblage

LATE PROTEROZOIC AND PALEOZOIC

PDSv amphibolite

PDSbp carbonaceous schist

PDSc marble

PDSs metaclastic rocks, quartzite, psammite

SYMBOLS

358 ± 1 U-Pb date (Ma) presented in this paper

355 ± 7 U-Pb date (Ma) from other sources

191.5 ± 1.1 ^{40}Ar-^{39}Ar date (Ma)

05MC023 metaplutonic geochemistry sample

05MC023 metavolcanic geochemistry sample

dextral strike-slip fault

thrust fault

normal fault

fault, unknown motion

area disturbed by placer operation

airstrip

Figure 3. *Representative greenstone of the Mendocina succession (DMFv), south of Mendocina Creek*

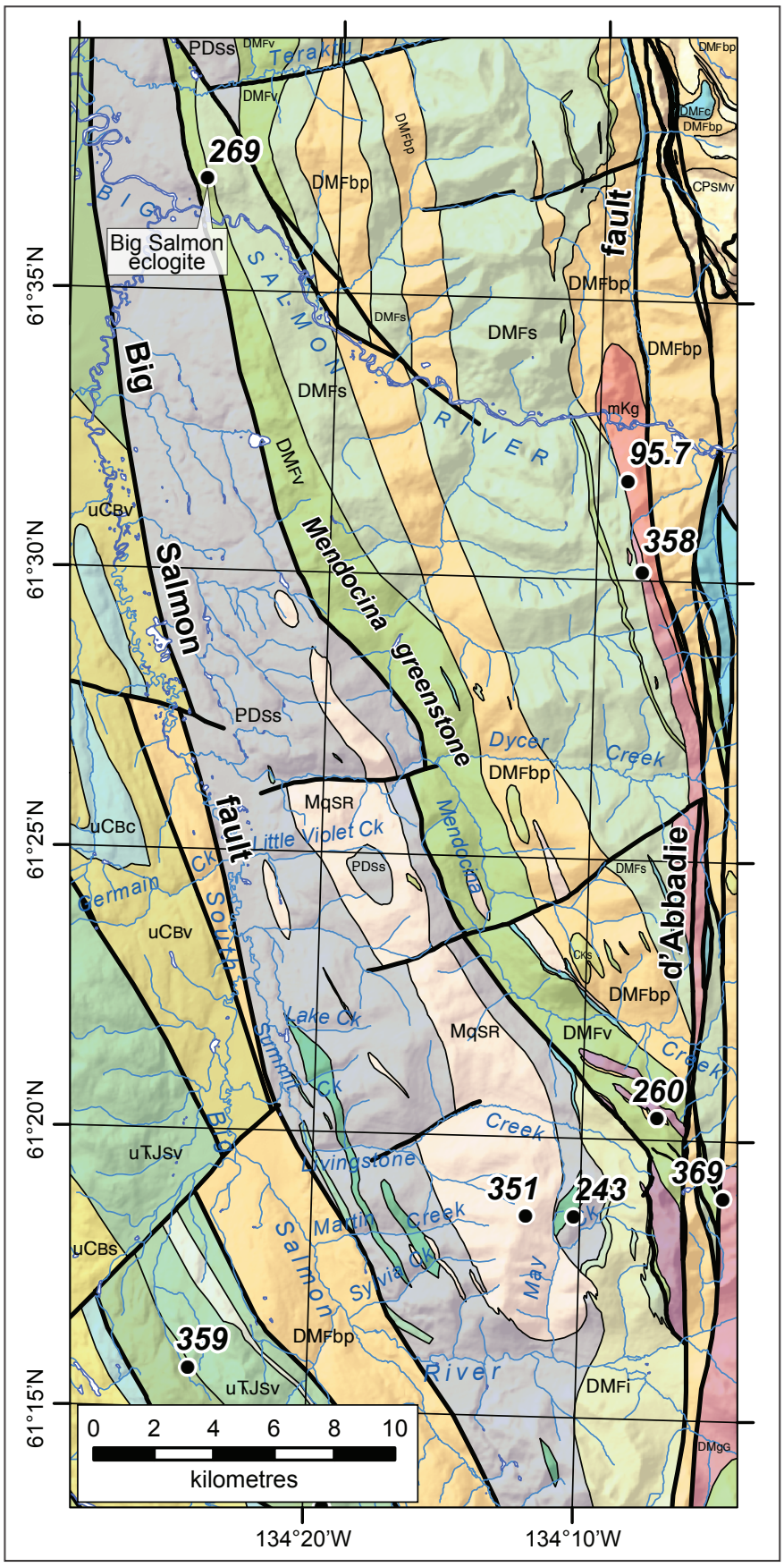

The **Last Peak succession** includes a belt of graphitic phyllite (Fig. 6a) and quartzite that progresses to the northeast into micaceous quartzite (Fig. 6b), mica schist and quartzite (Fig. 2; Colpron, 2005a; 2017). Marble and strongly foliated greenstone (Fig. 6c,d) occur in discrete bands within the micaceous quartzite and in proximity to the d'Abbadie fault (DMFv, Fig. 2). Carbonaceous phyllite, with quartzite, chert and marble exposed east of the d'Abbadie fault were previously assigned to the Dycer Creek succession (Colpron, 2005a; Westberg, 2009; Westberg *et al.*, 2009). They are herein considered the eastern extension of the Last Peak succession (Fig. 2). The Livingstone Creek, Mendocina and Last Peak successions are all tentatively assigned to the regional Devonian-Mississippian Finlayson assemblage of the Yukon-Tanana terrane (Fig. 2; Colpron *et al.*, 2006, 2016b).

The stratigraphically (and structurally) highest unit in the Yukon-Tanana terrane of Livingstone Creek area comprises chloritic schist (Fig. 7a) intercalated with greenish-grey quartzite and minor grey phyllite, and is exposed on ridge tops east of the d'Abbadie fault in the central part of the map area (Fig. 2). These rocks were considered the highest units in the Dycer Creek succession by Colpron (2005a), and segregated as the "Quartzite-Greenstone" succession by Westberg (2009). The presence of Late Devonian detrital zircon in the quartzite suggests a possible correlation with the **Klinkit assemblage** (Colpron *et al.*, 2006). Regionally, the Klinkit assemblage unconformably overlies older (and usually more deformed) rocks

Figure 4. *Regional geology of the Yukon-Tanana terrane in the eastern Laberge map area (from Yukon Geological Survey, 2016). Eclogite occurrence along the Big Salmon River is indicated, as well as locations of U-Pb dates from this study and Breitsprecher and Mortensen (2004). See Figure 2 for map legend.*

Figure 5. *Ultramafic massif at the headwaters of Livingstone Creek (DMFum). View is to the south-southeast. Field of view is ~3 km in width.*

Figure 6. *Representative lithology of the Last Peak succession:* ***(a)*** *carbonaceous and calcareous phyllite from Dycer Creek (DMFbp);* ***(b)*** *micaceous quartzite north of Dycer Creek (DMFs);* ***(c)*** *strongly transposed greenstone north of Dycer Creek (DMFv); and* ***(d)*** *contact between marble (left foreground) and greenstone (right foreground) is locally mineralized with pyrrhotite.*

of the Snowcap and Finlayson assemblages. Strongly foliated arkosic grit and polymictic conglomerate north of Mendocina Creek and west of the d'Abbadie fault were initially described as part of the Last Peak succession (Fig. 7b; Colpron, 2005a). These rocks resemble conglomerate typical of the basal Klinkit assemblage (Colpron *et al.*, 2006) and are also herein tentatively correlated with the Klinkit assemblage (Fig. 2).

There are a number of granitoids in the map area. Rocks of the Last Peak succession were intruded by moderately to strongly foliated, K-feldspar augen, two-mica metagranite that forms a narrow belt of exposures along the western edge of the d'Abbadie fault zone (Fig. 2). The metagranite is commonly protomylonitic to locally ultramylonitic near, and within the fault zone (Fig. 8). It is tentatively assigned to the **Grass Lakes plutonic suite** based on its Early Mississippian age (358 ± 1 Ma, *see* below; Colpron *et al.*, 2016a,b). Finer grained, strongly foliated to gneissic metagranite and metagranodiorite that intruded rocks of the Snowcap and Finlayson assemblages are assigned to the **Simpson Range plutonic suite** (Fig. 2; Colpron, 2005b; Colpron *et al.*, 2016a,b), including the large 351 ± 1 Ma pluton in the centre of the map area (*see* below for geochronology).

Variably (but generally weakly) foliated, medium to coarse-grained, two-mica granite occurs as small bodies and dikes throughout the area (Colpron, 2005b). One of these yielded a Permian age (*ca.* 260 Ma, *see* "U-Pb Geochronology" section below) suggesting that it may correlate with the **Sulphur Creek plutonic suite** (Mortensen, 1990; Colpron *et al.*, 2016a,b). The youngest known intrusive in the Livingstone Creek area is a fine to medium-grained, weakly foliated to protomylonitic biotite granite exposed along the western edge of the d'Abbadie fault zone north of Dycer Creek (Fig. 2; Last Peak granite of Harvey *et al.*, 1997; Gallagher, 1999; Colpron, 2005a). Gallagher (1999) reported a U-Pb monazite date of *ca.* 96 Ma for this granite (Fig. 4). Along its western edge, the granite intruded older, Mississippian augen metagranite; it becomes progressively more foliated towards the d'Abbadie fault to the east. Based on its age and composition, this pluton has been assigned to the 103-94 Ma **Seagull suite** (Colpron *et al.*, 2016a,b).

Rocks of the Yukon-Tanana terrane are strongly deformed by at least three phases of folds and foliation development. The second phase of deformation resulted in development of the dominant, regional, pervasive transposition foliation and is axial planar to tight to isoclinal folds. The transposition foliation and the main lithological contacts generally strike northwest and dip moderately to the southwest in the western part of the map area, whereas the dip becomes steep to moderate northeast of Mendocina Creek. West of d'Abbadie fault, most lithological contacts are potentially faulted, although only those contacts with clear fault relationships are shown on the map (Fig. 2). East of d'Abbadie fault, the foliation dips gently to the west-northwest. The dominant foliation is everywhere folded by northeast-verging open folds (Colpron, 2005b).

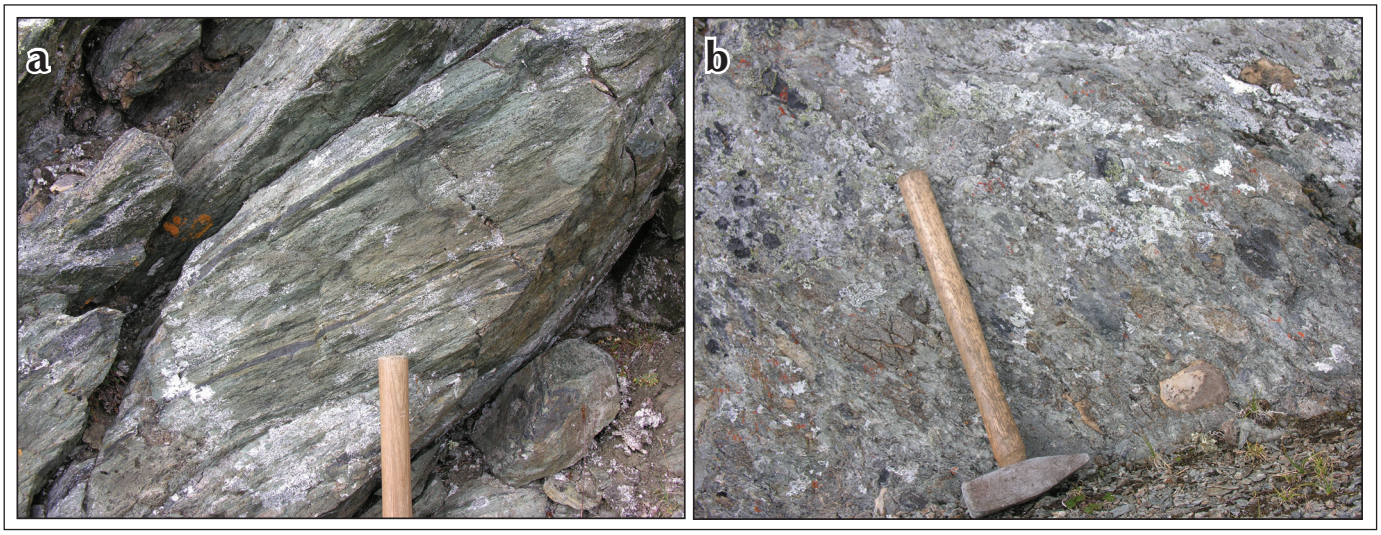

Figure 7. (a) *Greenstone of the Klinkit assemblage east of the d'Abbadie fault (CKv).* ***(b)*** *Polymictic conglomerate tentatively correlated with the basal Klinkit assemblage, west of d'Abbadie fault (CKs).*

Figure 8. *Mylonitic augen metagranite of the Grass Lakes suite (DMgG) west of the d'Abbadie fault and north of Dycer Creek.*

Yukon-Tanana terrane in the Livingstone Creek area was metamorphosed under medium to high-pressure (7-17 kbar) greenschist to amphibolite facies conditions (Hansen, 1992). Permian (*ca.* 270-265 Ma) eclogite and blueschist are locally preserved north and south of the area (Creaser *et al.*, 1997; Erdmer *et al.*, 1998; Petrie *et al.*, 2015, 2016). Occurrences of Na-amphibole, Na-pyroxene and phengite suggest the Livingstone Creek area probably experienced similar high-pressure conditions (Hansen, 1992; and our limited observations below). In the St. Cyr area to the south, Petrie *et al.* (2015, 2016) documented an early amphibolite facies metamorphism, overprinted by eclogite facies (up to 20 kbar; *ca.* 270-265 Ma), and then retrogressed to amphibolite facies. Early Jurassic (*ca.* 195-190 Ma) mica cooling ages in the Yukon-Tanana terrane of the Livingstone Creek area place a lower limit on the timing of amphibolite facies retrograde metamorphism (Fig. 2; Hansen *et al.*, 1989, 1991; Breistprecher and Mortensen, 2004).

The d'Abbadie fault is a vertical, north-striking, brittle-ductile fault zone approximately 1 km in width (Fig. 2). Kinematic indicators consistently demonstrate dextral strike-slip motion (Mercier, 2011). Mylonitic rocks are spatially associated with occurrences of the *ca.* 96 Ma Last Peak granite (Gallagher, 1999) and generally overprinted by cataclasite, suggesting that ductile deformation is in part Late Cretaceous. The Big Salmon fault to the west is not observed but is inferred to be of similar style and timing as the d'Abbadie fault.

VTEM™ PLUS GEOPHYSICAL SURVEY

Geotech Ltd. carried out a helicopter-borne geophysical survey over the Livingstone Creek area between March 17th and June 21st, 2016. The survey was commissioned by YGS and co-funded by the Canadian Northern Economic Development Agency. The Geological Survey of Canada (GSC) contributed expertise in designing the survey and overseeing data acquisition and processing. The survey results were jointly released by YGS and GSC in two open file reports (Boulanger *et al.*, 2016a,b).

Principal geophysical sensors included a versatile time-domain electromagnetic (VTEM™ Plus) system and horizontal magnetic gradiometer with two cesium sensors. Ancillary equipment included a GPS navigation system and a radar altimeter. The survey was flown in an east-west direction (N090° azimuth), with traverse line spacing of 200 m. Tie lines were flown perpendicular to the traverse lines at a spacing of 1200 m. A total of 4227 line-kilometres of geophysical data were acquired during the survey. Detailed specifications of the survey and data processing are given in the technical report that accompanies the open files (Boulanger *et al.*, 2016a,b).

The residual total magnetic intensity map illustrates two belts of well-defined magnetic lows that directly correspond with the d'Abbadie and Big Salmon fault zones, respectively (Fig. 9). There are a number of generally linear-trending, strong magnetic highs. The largest is a northwest-trending linear high (A on Fig. 9) extending from the South Big Salmon River, west of the d'Abbadie fault, to the western side of the Mendocina valley. South of Livingstone Creek, this high diverges into two prongs. The eastern prong corresponds to the large ultramafic massif at the headwaters of Livingstone and May creeks (Figs. 2 and 5; UM on Fig. 9), whereas the western prong coincides with the contact between the Livingstone Creek and Snowcap successions (Figs. 2 and 9). Along the northwest trend of the large linear magnetic high (northwest of A on Fig. 9), it coincides with the eastern edge of the Mississippian pluton (patterned area on Fig. 9); the high may represent magnetite enrichment along the transposed intrusive contact, or perhaps buried ultramafic rocks. West of the pluton, a series of narrow discontinuous magnetic highs are generally parallel to the contact with the pluton (B on Fig. 9), and are

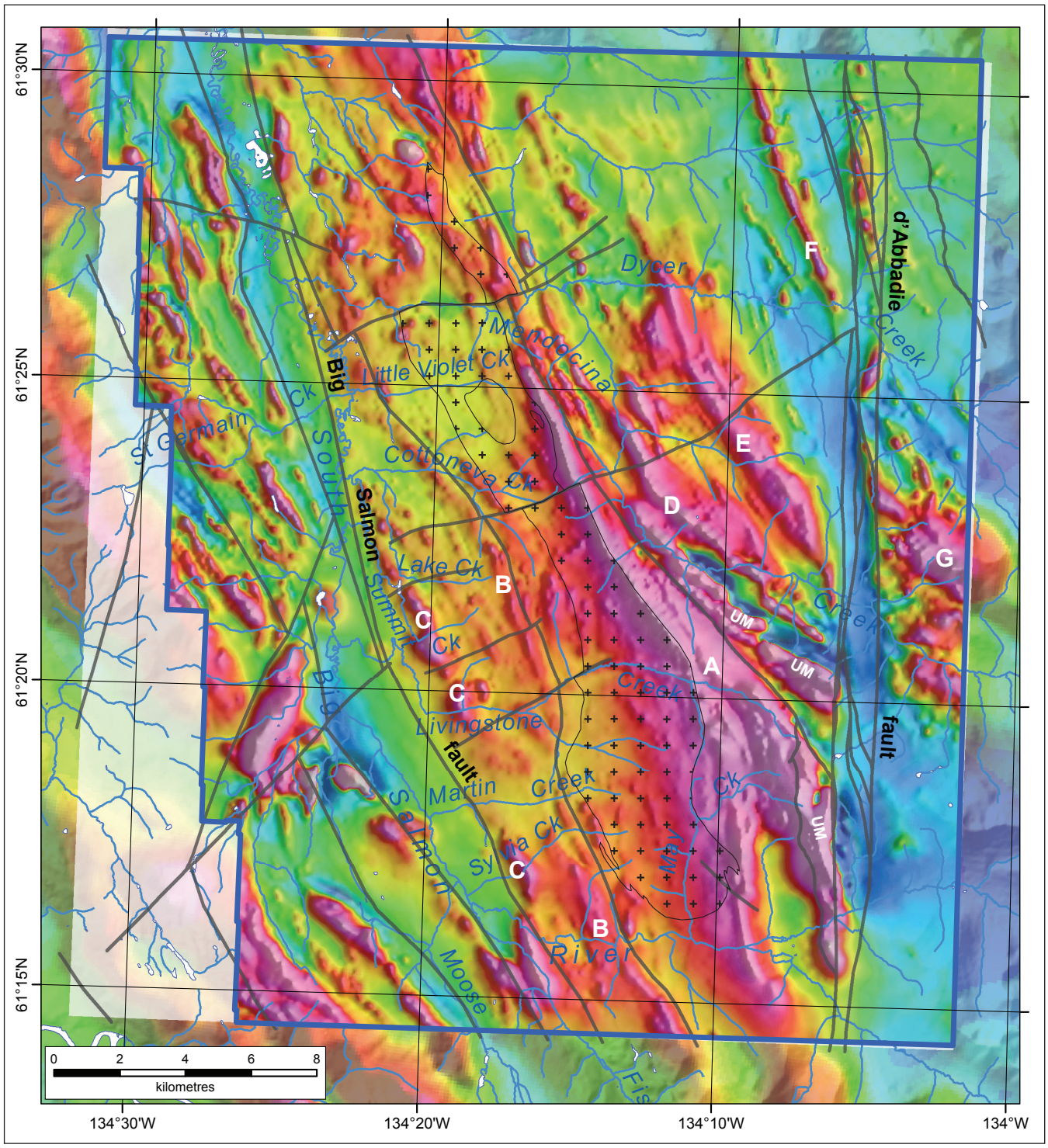

Figure 9. *Residual total magnetic intensity map of the Livingstone Creek area. The detailed survey (inside blue outline; Boulanger et al., 2016a,b) is superimposed on the regional aeromagnetic compilation of Hayward and Oneschuk (2011). Faults (solid grey lines) and the large Mississippian pluton (+ pattern) from Figure 2 are shown for reference. Known exposures of ultramafic rocks (UM) are also indicated. See text for explanations of magnetic anomalies labeled A to G.*

interpreted to occur along the western edge of a regional structural lineament within the Snowcap rocks (Fig. 2). The discontinuous highs that occur parallel to, and east of the Big Salmon fault between Sylvia and Lake creeks (C on Fig. 9), coincide with greenstone exposures in the Snowcap assemblage (Fig. 2).

North of the headwaters of Livingstone Creek, strong west to northwest-trending magnetic highs (UM on Fig. 9) coincide with ultramafic bodies. In the east-central part of the map area, a northwest-trending magnetic high (D on Fig. 9) marks the contact between the Mendocina greenstone and graphitic phyllite and marble of the Last Peak succession (Fig. 2). The strong northwest-trending magnetic high located between Mendocina and Dycer creeks (E on Fig. 9) occurs within graphitic phyllite of the Last Peak succession and is presently unexplained (*see* Mineral Potential section below for further discussion). The narrow magnetic high that parallels the d'Abbadie fault north of Dycer Creek in the northeast part of the map area (F on Fig. 9) corresponds with a narrow band of sheared greenstone that locally contains disseminated pyrrhotite where it is in contact with marble (Fig. 6c,d). The strong magnetic high, located east of the d'Abbadie fault (G on Fig. 9), corresponds mainly with greenstone exposures of the Klinkit assemblage (Fig. 2); two smaller highs to the south of locale G, flanking Dycer Creek, are currently unexplained by published maps (Colpron, 2005a; Westberg, 2009).

The trends in the magnetic data coincide very well with mapped geology (Colpron, 2005a); however, the geophysical data are particularly useful in refining contact locations and enhancing interpretation of the bedrock geology (Fig. 2; Colpron, 2017). For this purpose, we gridded the final levelled residual total magnetic intensity data (excluding the tie lines) using the Geosoft™ bi-directional gridding algorithm with a cell size of 50 m, which is ¼ of the nominal line spacing. Azimuths of 160/340 and 020/200 were used for the bi-directional gridding. The resultant grids are rotated to the pole and the tilt derivatives calculated (Fig. 10; Appendix 1a). Shading uses the generalized derivative operator of Cooper and Cowan (2011) with either a 160 or 020 direction.

The resultant image of the 160/340 bi-directional gridding (Fig. 10) emphasizes the strong northwest-striking fabric in metamorphic rocks of the Yukon-Tanana terrane (Colpron, 2005a,b). In many places, the strong northwest lineaments are disrupted or bent along northeast-trending discontinuities, some of which coincide with mapped late brittle faults (Colpron, 2005a; examples are indicated by arrows on Fig. 10). We further discuss potential implications of these northeast-trending features in the Mineral Potential section below.

The electromagnetic data are dominated by large, strong conductive areas that correspond with exposures of graphitic phyllite (hatched area on Fig. 11). Northeast of Mendocina Creek, on both sides of d'Abbadie fault, the corresponding graphitic phyllite is assigned to the Last Peak succession (Fig. 2). The strong conductor along the western side of the South Big Salmon River is believe to also represent graphitic rocks; Simard (2003) mapped a single outcrop of graphitic siltstone in this region, north of St. Germain Creek.

On a smaller scale, there are also three strong, linear electromagnetic conductors (locations 1-3 on Fig. 11) that do not appear to be related to graphitic rocks. East of the large Mississippian pluton (patterned area on Fig. 11), a strong linear conductor extends for approximately 15 km between the South Big Salmon River and Cottoneva Creek (1 on Fig. 11), and straddles the fault inferred from the magnetic data. This conductor appears to be concordant with the transposition foliation, and dips steeply to the west, as suggested by the westward shift of the anomaly between early and late channels (Boulanger *et al.*, 2016a,b). It is notable that rocks corresponding with this conductor are situated above or upstream of many of the creeks that have seen placer production (shown in red on Fig. 11). According to Boulanger *et al.* (2016a,b) the top of this conductor occurs at a depth of 55-70 m.

Another notable linear electromagnetic conductor occurs north of Dycer Creek in the northeastern part of the Livingstone Creek area, and extends for more than 6 km to the northern edge of the survey area (2 on Fig. 11). This conductor is nearly vertical and appears to be concordant with the transposition foliation. It coincides with occurrences of strongly sheared greenstone in the Last Peak succession (Figs. 2 and 6c,d), and local occurrences of pyrrhotite mineralization associated with this unit (*see* below for further discussion). A vein system with galena mineralization coincides with the eastern flank of this conductor (Yukon MINFILE 105E 064; Fig. 11). This conductor also coincides with a magnetic high (F on Figs. 9 and 10) and is modeled to occur at a depth of 70-100 m (Boulanger *et al.*, 2016a,b).

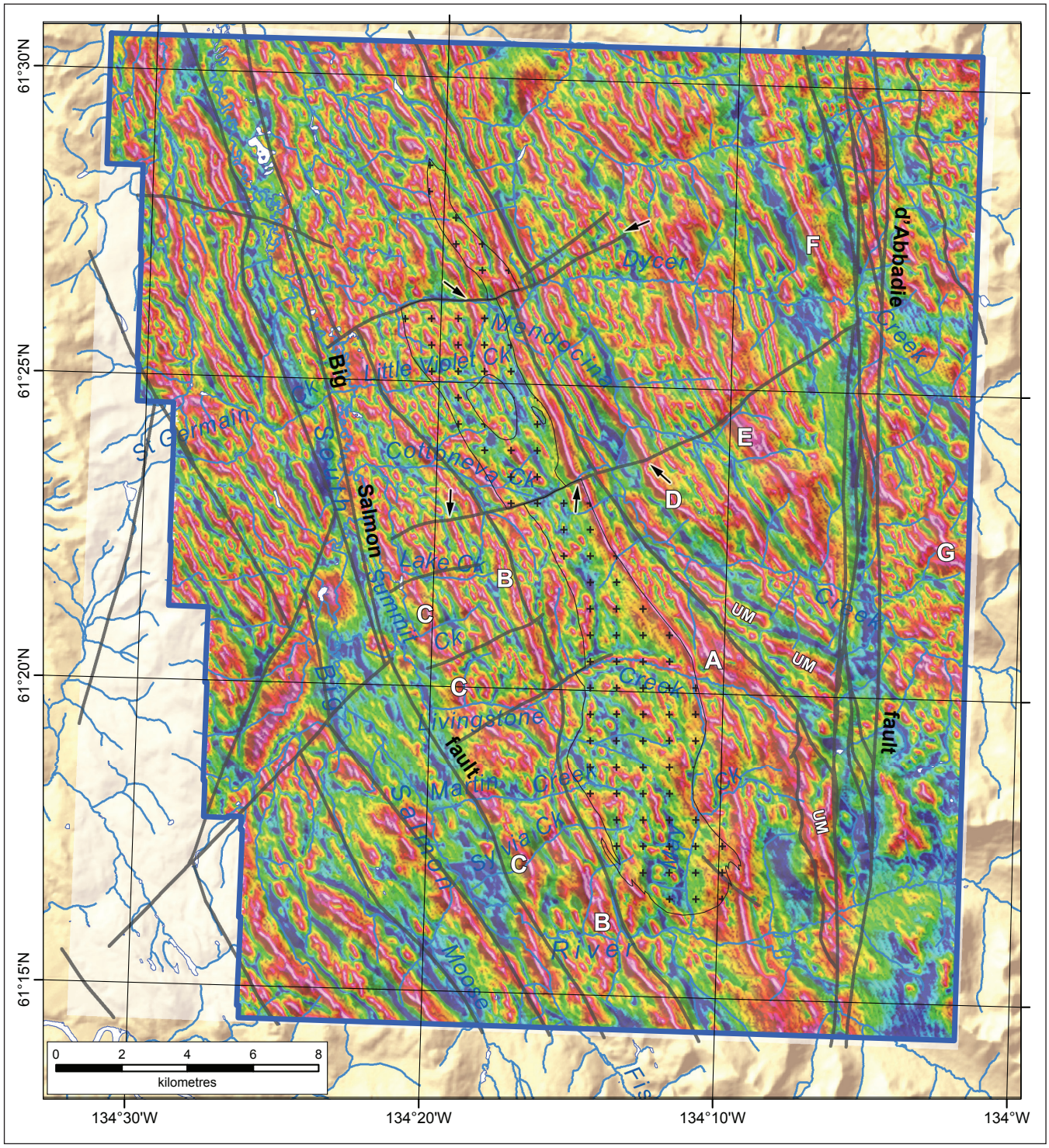

Figure 10. *Bi-directional gridded, rotated-to-pole, tilt derivative of the magnetic intensity (see Appendix 1). Faults (solid grey lines) and the large Mississippian pluton (+ pattern) from Figure 2 are shown for reference. Features labeled on Figure 9 are indicated on this map as well. Arrows point to truncations of the prominent northwest-trending magnetic fabric along weaker northeast trends, some of which coincide with mapped brittle faults (Colpron, 2005a)*

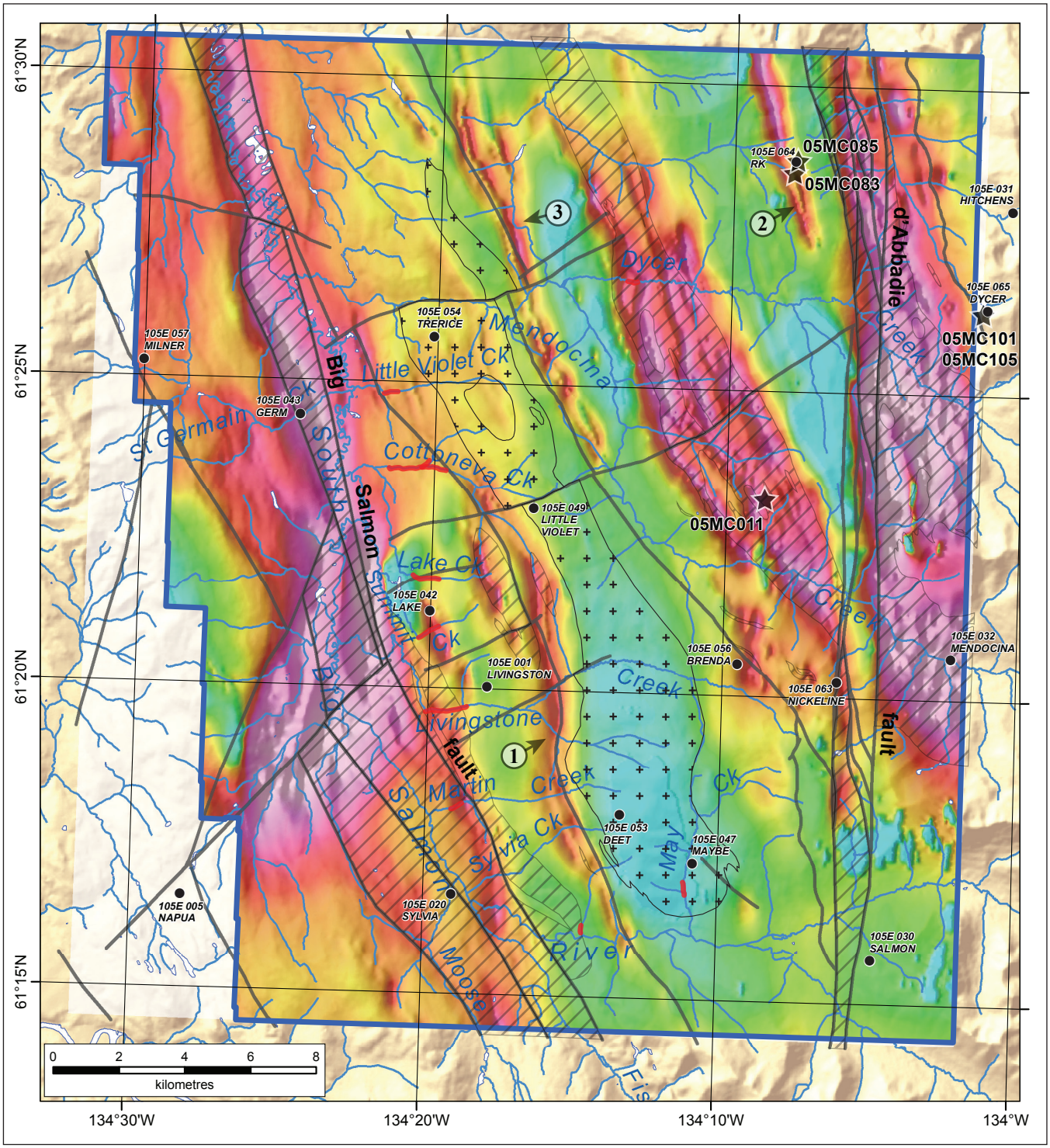

Figure 11. *Apparent electromagnetic conductivity, based on decays of mid-channels (15-30; Boulanger et al., 2016a,b). Faults (solid grey lines) and the large Mississippian pluton (+ pattern) from Figure 2 are shown for reference. Hatched areas indicate extent of mapped graphitic lithology at surface (from Fig. 2). Circled numbers 1 to 3 correspond to conductors discussed in the text. Mineral occurrences are denoted by black dots; the associated number and occurrence name refer to Yukon MINFILE (2016). Stars illustrate locations of assay samples reported on Table 5. Areas disturbed by placer mining activity are designated by red heavy lines along creeks.*

Finally, another linear electromagnetic conductor extends for approximately 12 km in the north-central part of the survey area (3 on Fig. 11). The interpretation of this conductor is enigmatic due to poor exposure in this part of the map area. The conductor appears to be situated in the immediate hangingwall of an east-dipping fault that bounds the western margin of the Mendocina greenstone (Figs., 2 and 11; Boulanger *et al.*, 2016a,b). Depth to the top of this conductor is estimated at 70-90 m.

GEOCHEMISTRY

A total of 41 meta-igneous rocks from the Yukon-Tanana terrane in the Livingstone Creek area were collected during field mapping in 2004-2005. They were analyzed for major and trace elements at Activation Laboratories in Ancaster, Ontario (*see* Tables 1 and 2 at end of paper). Of these, 24 samples are from rocks of inferred volcanic protoliths (and cogenetic intrusions; Table 1), and 17 samples are from metaplutonic bodies and dikes that intruded the metasedimentary and metavolcanic rocks (Fig. 2; Table 2). Five samples of metavolcanic rocks from the Mendocina, Last Peak and Klinkit successions were also analyzed for Nd and Hf isotopes (Table 3; *see* Appendix 2 for methods).

METAVOLCANIC ROCKS

Samples of metavolcanic rocks (and related mafic intrusive rocks) were collected from the Snowcap and Klinkit assemblages, and the Livingstone Creek, Mendocina and Last Peak successions (Finlayson assemblage).

Snowcap assemblage

Four samples of mafic schist and amphibolite of the Snowcap assemblage were analyzed (Fig. 1; Table 1). The samples have SiO_2 of 45-53% and a trace element character of sub-alkaline to alkaline basalt (Fig. 12a,b).

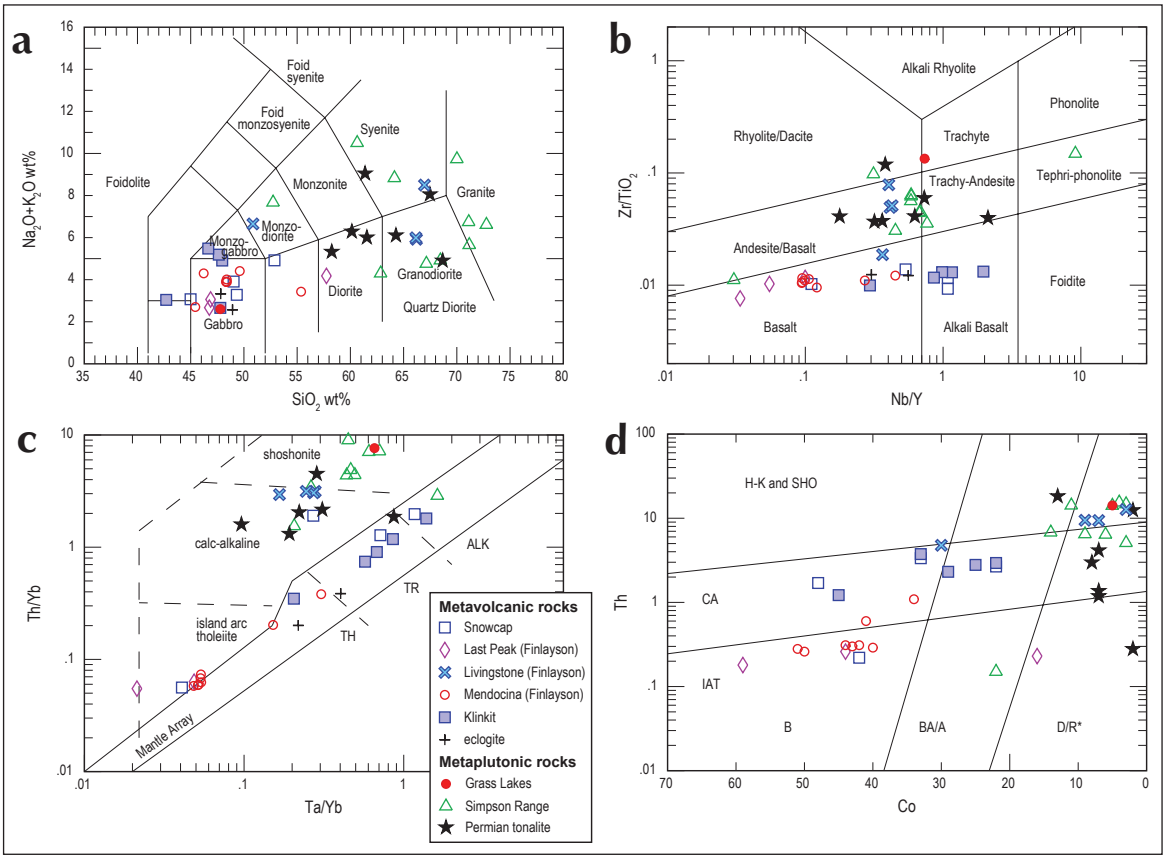

Figure 12. *Geochemical classification diagrams for meta-igneous rocks of the Livingstone Creek area.* ***(a)*** *Total alkalis vs. silica diagram of Le Bas et al. (1986).* ***(b)*** *Pearce (1996) modifications of the Zr/TiO_2 vs. Nb/Y diagram of Winchester and Floyd (1977).* ***(c)*** *Th/Yb vs. Ta/Yb discrimination diagram of Pearce (1982). TH=tholeiite; TR=transitional; ALK=alkaline.* ***(d)*** *Th vs. Co discrimination diagram of Hastie et al. (2007). B=basalt; BA/A=basaltic andesite/andesite; CA=calc-alkaline; D/R*=dacite/rhyolite (including latite and trachyte); H-K=high-K calc-alkaline; IAT=island arc tholeiite; SHO=shoshonite.*

Discrimination diagrams (Fig. 13) and trace element patterns (Fig. 14a) show that two Snowcap samples (04MC115, 04MC 146) have ocean island basalt (OIB) to transitional affinities, one sample (02MC124) appears more primitive with a normal mid-ocean ridge basalt (NMORB) signature, and one sample (04MC108) is of calc-alkaline affinity. The two samples with OIB signature compare well with Snowcap amphibolite from the Glenlyon area to the north (Figs. 1 and 14a; Piercey and Colpron, 2009). The other two samples show more affinity to the Mendocina or Livingstone Creek successions described below and may be related to them.

Livingstone Creek succession

Four samples of chloritic and feldspathic schist interpreted to be derived from a volcaniclastic protolith were analyzed (Colpron, 2005b). Three of the four samples have SiO_2 of 66-67% and low Co content, suggesting a felsic protolith (Fig. 12a,d; Table 1). The fourth sample (04MC056) has SiO_2 and Co contents consistent with a basaltic protolith (Table 1; Fig. 12a,d). On trace element classification diagrams, all Livingstone Creek samples plot as calc-alkaline basaltic andesite to basalt (Fig. 12b,c). On discrimination diagrams, these samples consistently plot in the calc-alkaline fields (Fig. 13), and their trace element patterns display negative Nb and Ti anomalies characteristic of calc-alkaline arc rocks (Fig. 14c). This geochemical signal is similar to intermediate to felsic arc volcanic rocks documented in other parts of the Yukon-Tanana terrane (*e.g.*, Colpron, 2001; Piercey *et al.*, 2006).

Mendocina succession

Seven samples of massive greenstone and one of coarse-grained metagabbro (04MC065) were analyzed (Table 1). They have SiO_2 of 45-55%, and trace element signatures characteristic of primitive, tholeiitic basalt (Fig. 12). They plot in the NMORB to enriched mid-ocean ridge basalt (EMORB) fields on discrimination diagrams (Fig. 13) and display trace element patterns characteristic of NMORB and EMORB signatures as well (Fig. 14b). Two samples of Mendocina greenstone have juvenile εNd_t (+4.2-4.8) and εHf_t (+5.0-6.5; Table 3, 04MC080-2 and 05MC018) consistent with derivation from depleted mantle sources. These primitive signatures and the association of ultramafic rocks with the Mendocina greenstone (Fig. 2) are compatible with emplacement in an ocean floor setting.

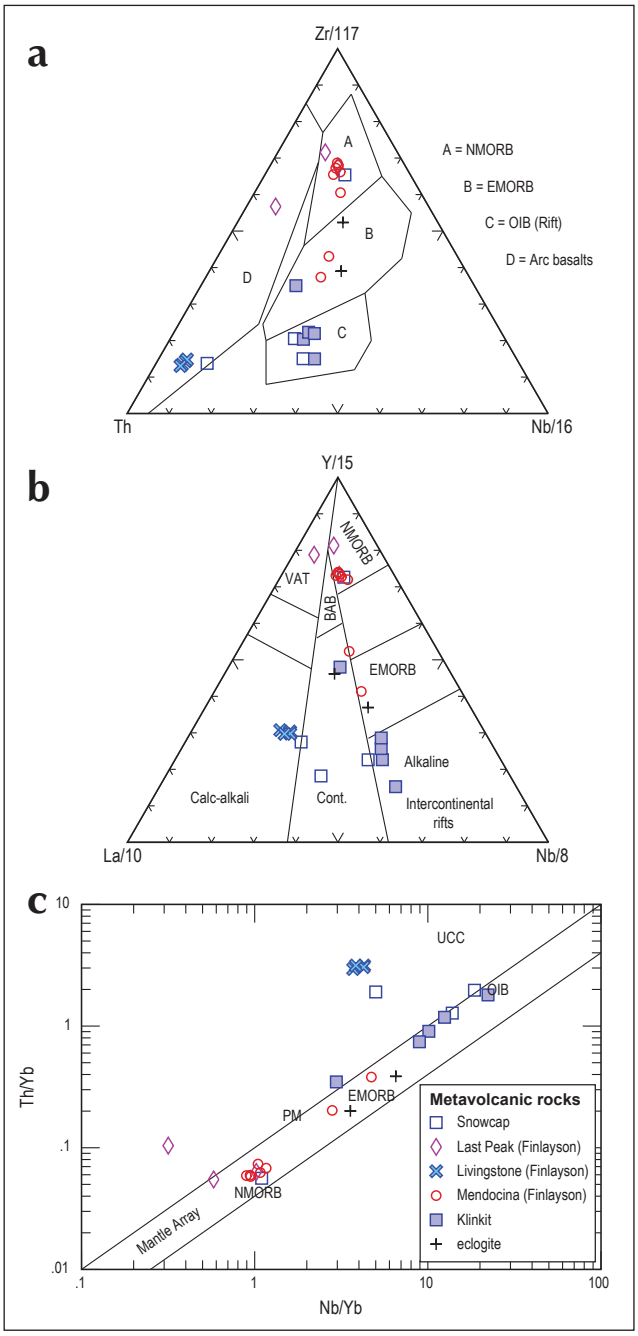

Figure 13. *Trace element discrimination diagrams for mafic and intermediate rocks of the Yukon-Tanana terrane in the Livingstone Creek area.* ***(a)*** *Th–Zr/117–Nb/16 diagram of Wood (1980).* ***(b)*** *La/10–Y/15–Nb/8 diagram of Cabanis and Lecolle (1989).* ***(c)*** *Th/Yb vs. Nb/Yb diagram of Pearce and Peate (1995). BAB = back-arc basin; Cont. = continental basalt; EMORB = enriched mid-ocean ridge basalt; NMORB = normal mid-ocean ridge basalt; OIB = ocean-island basalt; PM = primitive mantle; UCC = average upper continental crust; VAT = volcanic arc tholeiite.*

The distinct belt of Mendocina greenstone mapped in the Livingstone Creek area extends northwestward to the Big Salmon River where a *ca.* 269 Ma eclogite occurrence is exposed (Fig. 4; Creaser *et al.*, 1997; 1999). The geochemistry of the Big Salmon eclogite (*aka* Last Peak eclogite) suggests an EMORB affinity (Creaser *et al.*, 1999), and is comparable to more enriched samples from the Mendocina succession (Figs. 13 and 14b). However, the Big Salmon eclogite has more juvenile εNd_t of +7.3 (Creaser *et al.*, 1999) compared to our Mendocina samples (Table 3). The bulk of the Mendocina samples also have NMORB trace element compositions similar to eclogite from the St. Cyr 'klippe' to the southeast (Fig. 1), also dated at 271-265 Ma (Petrie *et al.*, 2015; 2016). Occurrences of blue, sodic amphibole in some of the Mendocina samples (Fig. 15) suggests that rocks in the Livingstone Creek area may also have experienced high-pressure metamorphism (Hansen, 1992).

Last Peak succession

Greenstone is scarce in the Last peak succession and only 3 samples were analyzed (Table 1). Two samples are from highly strained greenstone bands (Fig. 6c) in micaceous quartzite and minor marble north of Dycer Creek, near the d'Abbadie fault, whereas one sample (05MC042) is from a small greenstone lens in graphitic phyllite south of Dycer Creek (Fig. 2). The two northern samples have SiO_2 of 47% and trace element characteristics of sub-alkaline basalt (Fig. 12). The southern sample has a higher SiO_2 content of 57% but plots in tholeiitic fields on discrimination diagrams (Figs. 12 and 13). The northern samples have depleted trace element patterns characteristic of NMORB, whereas the more felsic sample (05MC042) exhibits island arc tholeiite affinities (Figs. 13 and 14b). One sample of amphibolite from the Last Peak succession (05MC086-2) has juvenile εNd_t (+4.7) and

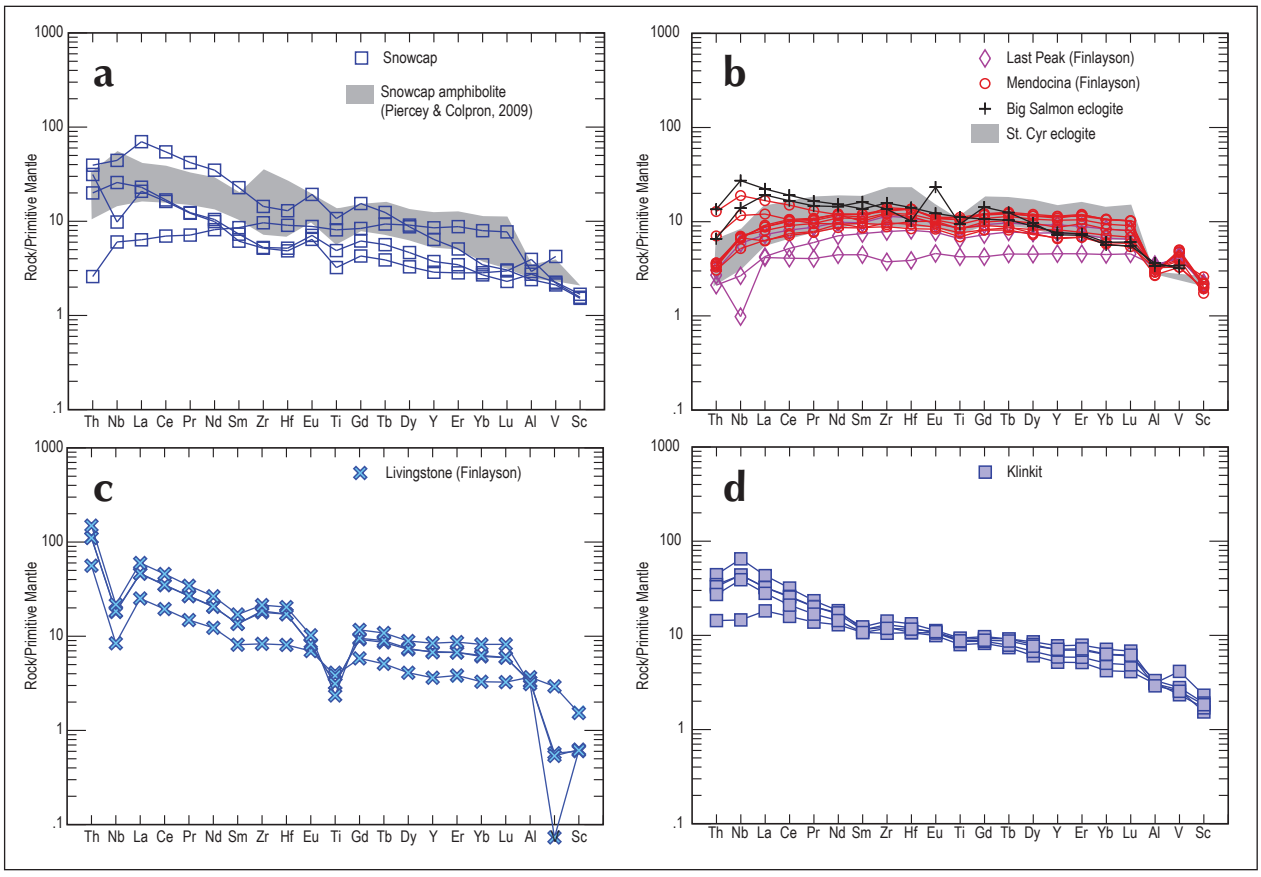

Figure 14. *Immobile trace element patterns normalized to primitive mantle values (Sun and McDonough, 1989) for metavolcanic rocks of the Yukon-Tanana terrane.* ***(a)*** *Comparison of metabasite of the Snowcap assemblage in Livingstone Creek and Snowcap amphibolite from Glenlyon area (grey shading, after Piercey and Colpron, 2009).* ***(b)*** *Comparison of greenstone of the Mendocina and Last Peak successions, with two eclogite samples collected approximately 13 km northwest of the map area along the Big Salmon River (Fig. 4; data from Creaser et al., 1999). Grey shading shows range of eclogite from the St. Cyr area (data from Petrie et al., 2015).* ***(c)*** *Intermediate metavolcanic and metavolcaniclastic rocks of the Livingstone Creek succession.* ***(d)*** *Mafic metavolcanic rocks of the Klinkit assemblage.*

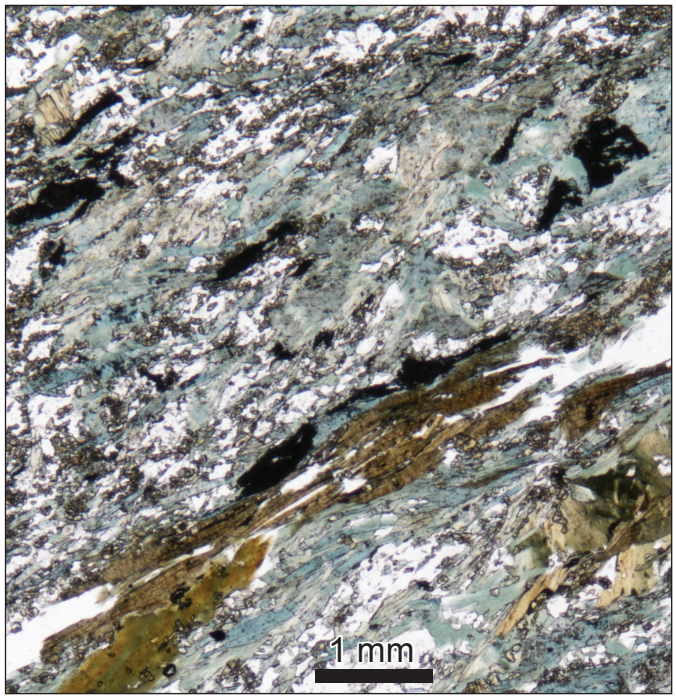

Figure 15. *Photomicrograph of blue sodic amphibole from greenstone of the Mendocina succession (sample 05MC018, Fig. 2; Table 1). Cross-polarized light.*

εHf_t (+6.6) comparable with the Mendocina samples (Table 3). The two northern samples closely match the more depleted samples from the Mendocina greenstone and could be genetically related (feeder dikes?).

Klinkit assemblage

Four samples of greenstone were collected from the structurally highest level, between Mendocina and Dycer creeks, east of the d'Abbadie fault (Fig. 2). These rocks are correlated with the Klinkit assemblage (Colpron *et al.*, 2006, 2016b; the Quartzite-Greenstone succession of Westberg, 2009). A sample of metagabbro (05MC096) that intruded marble north of Dycer Creek is also considered part of this suite (Table 1). All Klinkit assemblage samples have SiO_2 of 43-48% and trace element concentrations consistent with alkali basalt of OIB to EMORB affinities (Figs. 12-14d). Two samples (05MC189, 05MC217) yielded εNd_t (+1.5-2.0) and εHf_t (-0.4- +1.9) that are closer to chondritic values (Table 3). These lower values could indicate crustal contamination. However, the absence of negative Nb anomalies relative to Th and La in their trace element patterns is inconsistent with this interpretation (Fig. 14d). We favour derivation from lithospheric mantle sources with a history of LREE-enrichment. These geochemical signatures are comparable to other alkalic rocks in the Klinkit assemblage elsewhere in the Yukon-Tanana terrane (Colpron, 2001; Simard *et al.*, 2003, 2007; Piercey *et al.*, 2006).

METAPLUTONIC ROCKS

Samples of metaplutonic rocks were collected from the large intrusion in the centre of the map area and other smaller bodies assigned to the Simpson Range plutonic suite, augen granite along the west flank of the d'Abbadie fault (Grass Lakes suite?), and from Permian two-mica granite dikes throughout the map area (Fig. 2; Table 2).

Grass Lakes and Simpson Range suites

Only one sample from the Early Mississippian augen granite, flanking the western edge of the d'Abbadie fault zone, was analyzed (Fig. 2; Table 2). The sample (05MC121) has unusually low SiO_2 content (48%) for the granitic lithology observed along this belt, but shows an evolved composition on trace element diagrams (Fig. 12) consistent with the mapped lithology. The low SiO_2 content may be a result of alteration of this sample along the fault. The sample plots as a calc-alkaline to shoshonitic volcanic arc rock on trace element diagrams (Figs. 12, 16 and 17a,c).

Nine samples of metagranodiorite, diorite and tonalite were analyzed from the main Mississippian pluton and smaller bodies of the Simpson Range suite west of d'Abbadie fault (Fig. 2; Table 2). Three other samples collected east of d'Abbadie fault in the northeastern corner of the map area are also assigned to the Simpson

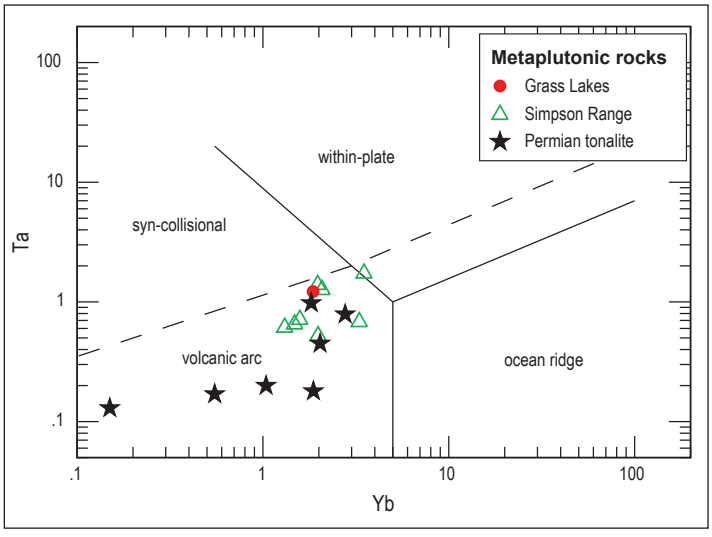

Figure 16. *Ta–Yb discrimination diagram for metaplutonic rocks of the Yukon-Tanana terrane in the Livingstone Creek area (after Pearce et al., 1984).*

Range suite. Most samples have SiO_2 content of 61-71% consistent with granodiorite to granite composition, although one sample plots as a monzodiorite (05MC023, SiO_2 53%; Fig. 12a). All samples plot in the volcanic arc field of the Ta/Yb diagram (Fig. 16). Most samples have trace element patterns characteristic of calc-alkaline, high-K to shoshonitic arc rocks (Fig. 17a,c). Sample 05MC023 has a more depleted pattern, typical of island arc tholeiite.

Permian intrusives (Sulphur Creek suite?)

Seven samples of felsic schist, two-mica granite, and tonalite from small bodies and dikes were sampled (Fig. 2; Table 2). One of these samples (04MC101-3) is dated at *ca.* 260 Ma (*see* below). All samples have a diorite to granodiorite (58-69% SiO_2), calc-alkaline composition typical of arc rocks (Figs. 12, 16 and 17b,d).

U-PB GEOCHRONOLOGY

We report the result of U-Pb dating of four meta-igneous rocks collected during mapping of the Livingstone Creek area (Fig. 2; Table 4). Two of the samples (04MC034-1 and 04MC101-3) were collected during regional mapping by M. Colpron in 2004 (Fig. 2; Colpron, 2005a). The other two samples (YT95-BS082 and YT96-BS093) were collected in the mid-1990s during the SNORCLE Lithoprobe program, as part of a graduate student mapping and research project (Gallagher, 1999; Carr *et al.*, 1999). These localities were revisited by M. Colpron and/or S.D. Carr in 2009-2010 to verify field relationships.

Sample preparation, analytical techniques and data reduction were carried out by S.D. Carr at Carleton University's Isotope Geochemistry and Geochronology Centre using methods described by Krogh (1973, 1982), Roddick (1987), Roddick *et al.* (1987) and Parrish *et al.* (1987).

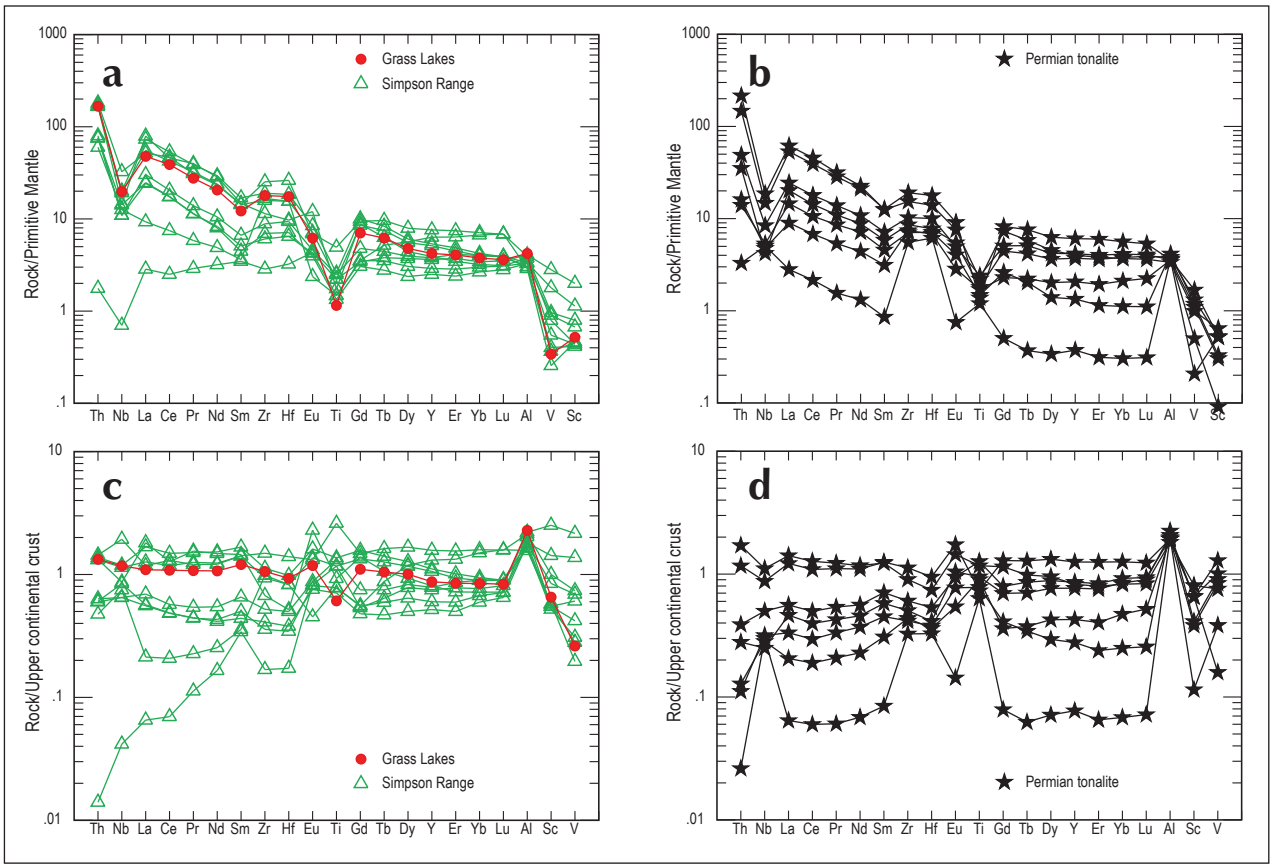

Figure 17. ***(a)*** *Immobile trace element patterns normalized to primitive mantle for Devonian-Mississippian granitoids.* ***(b)*** *Immobile trace element patterns normalized to primitive mantle for Permian granitoids. Primitive mantle values of Sun and McDonough (1989).* ***(c)*** *Immobile trace element patterns normalized to average upper continental crust for Devonian-Mississippian granitoids.* ***(d)*** *Immobile trace element patterns normalized to average upper continental crust for Permian granitoids. Upper continental crust values of McLennan (2001).*

YT95-BS082 – GRANITIC AUGEN ORTHOGNEISS

Map unit DMgG is a muscovite-biotite-bearing, granitic augen orthogneiss that borders the western side of the d'Abbadie fault zone, in the northern part of the map area (Figs. 2 and 8; Gallagher, 1999; Colpron, 2005a). It occurs as a <1 km-thick, steeply dipping sheet, extending for >15 km along a north or north-northwest strike (Fig. 2). Contacts between the orthogneiss, and transposed bedding and foliations within the Last Peak succession country rocks are concordant; there are no chilled margins or evidence of relict intrusive contacts (Gallagher, 1999, and references therein). The main foliation in the orthogneiss is a mylonitic C-plane (Fig. 8). Structural analysis by Gallagher (1999) indicates that the orthogneiss has undergone a complex general strain history with a significant component of dextral strike-slip motion, as well as boundary-parallel shortening and local west-side-down, dip-slip motion.

Zircon crystals are igneous, on the basis of morphology (*e.g.*, euhedral, doubly terminated bipyramids), but are generally of poor quality with cores. In contrast, there are some very small (*e.g.*, <64 µm) euhedral zircons that are of high quality and free of cores. Multigrain 149-200 µm and 105-149 µm-sized zircon fractions were analyzed and are highly discordant with $^{207}Pb/^{206}Pb$ ages of *ca.* 2000 and 1500 Ma (Table 4; Fig. 18a), indicating inherited Pb in xenocrystic cores. However, a fraction of <64 µm-sized zircons is free of cores and yields a concordant age of 357.8 Ma (Fig. 18b). An age assignment of 358 ± 1 Ma is based on data from this concordant fraction. The error is the average error of the $^{206}Pb/^{238}U$ and $^{207}Pb/^{235}U$ ages, rounded to 1 Ma. The 358 ± 1 Ma date is interpreted as the igneous crystallization age of the granite protolith. Based on this age, this granitic orthogneiss is considered part of the 365-357 Ma Grass Lakes plutonic suite (Colpron *et al.*, 2016a,b).

04MC034-1 – METAGRANODIORITE FROM LARGEST PLUTON

This sample was collected from the south end of the large pluton of foliated to gneissic, metagranite to metagranodiorite that intruded the Snowcap assemblage in the centre of the Livingstone Creek area (Fig. 2; Colpron, 2005a). This pluton occurs as a ~2 to 4 km-thick, steeply west-dipping granitoid sheet that extends ~20 km along a north-northwest strike. The dated metagranodiorite sample (Fig. 19), is a foliated, medium-grained, muscovite, biotite, clinozoisite and pyroxene (jadeite?)-bearing metagranodiorite with minor garnet, epidote and relict amphibole.

Zircon crystals are interpreted to be igneous on the basis of morphology (*e.g.*, euhedral, doubly terminated bipyramids) with internal regular or concentric oscillatory zoning (Fig. 18c inset). Three fractions of abraded zircon crystals were analyzed (Table 4; Fig. 18c). Fractions B, E and F were composed of one, two and four crystals, respectively. Data from these fractions are near concordant with 1.3%, 1.4% and 1.8% discordance, respectively (Table 4). The three $^{207}Pb/^{206}Pb$ ages range from 350.0 to 352.1 Ma. These data are consistent with the interpretation that the zircons do not have an inherited component of Pb, and have undergone a minor amount of Pb loss. The date for the rock is interpreted to be 351 ± 1 Ma. The date is based on the average $^{207}Pb/^{206}Pb$ age of the three zircon fractions. The error of 1 Ma is assigned on the basis of the overlap of the most concordant fraction E with the concordia curve (Fig. 18c).

The assigned date of 351 ± 1 Ma is interpreted as the crystallization age of a granodiorite protolith in the largest pluton of the Livingstone Creek area. It is assigned to the 357-345 Ma Simpson Range plutonic suite (Colpron *et al.*, 2016a,b). The date provides a minimum age for the Snowcap assemblage in the area, and is older than regional deformation and metamorphism in the Snowcap assemblage and this granitoid.

04MC101-3 – DEFORMED AND METAMORPHOSED FELSIC DIKE

Strongly foliated and lineated, yellow to orange-weathering, white to light green felsic schist occurs as 20 cm to 10 m-thick layers encased in black graphitic phyllite and dark green greenstone of the Mendocina succession (Fig. 20). At the outcrop scale, the contacts and foliation in the schist are concordant with those of adjacent rocks; however, at the scale of the ridge, the schist is discordant with the country rock. The schist is composed of predominantly fine-grained quartz and plagioclase with relict quartz and plagioclase phenocrysts that have undergone sericitic alteration (Fig. 20c). It contains 5% muscovite in the matrix, and minor pyrite. Cathode luminescence and backscatter images of zircons in grain mounts show concentric oscillatory zoning and euhedral bipyramidal morphology consistent with igneous crystals (inset Fig. 18d). On the basis of relict igneous textures (*i.e.*, plagioclase phenocrysts, igneous zircon) and discordance of the felsic schist contacts with those in the country rock (at the scale of tens of metres), the schist is interpreted as a metamorphosed and deformed felsic dike. It intruded the Mendocina succession, and was subsequently metamorphosed and deformed.

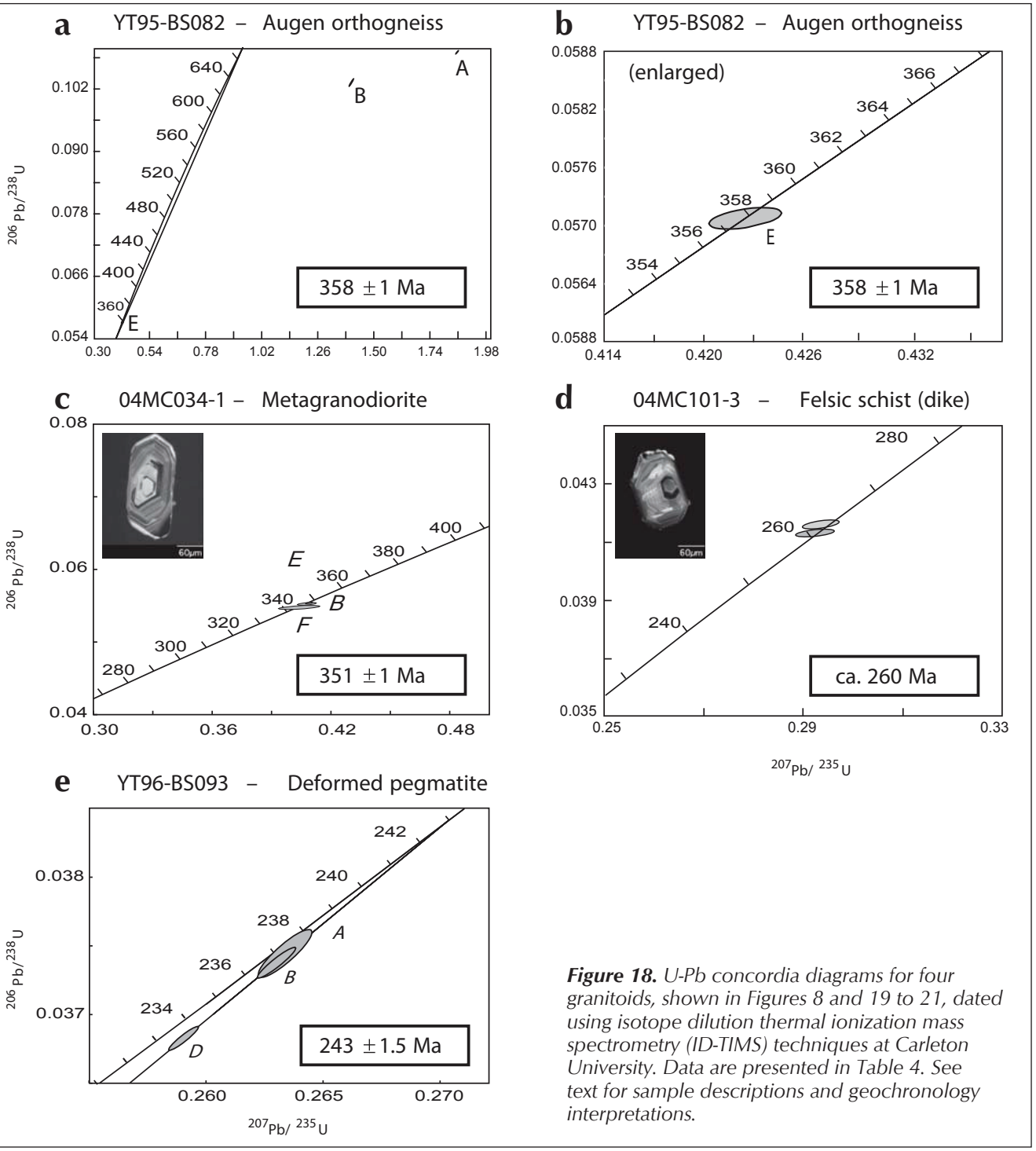

Figure 18. *U-Pb concordia diagrams for four granitoids, shown in Figures 8 and 19 to 21, dated using isotope dilution thermal ionization mass spectrometry (ID-TIMS) techniques at Carleton University. Data are presented in Table 4. See text for sample descriptions and geochronology interpretations.*

Most zircons are <100 μm in size. Two fractions of three and four abraded 74-105 µm-zircons were analyzed. Data are reversely concordant with -5.7% and -2.1% discordance, respectively (Table 4). The cause of the reverse discordance is unresolved. Further analyses are in progress; however, a provisional age of *ca.* 260 Ma is based on the $^{207}Pb/^{235}$ U ages of two fractions, and is interpreted to approximate the crystallization age of the rock. The *ca.* 260 Ma provisional date is interpreted as the crystallization age for this felsic dike. This age is equivalent to magmatism associated with the Klondike arc cycle and intrusions of the Sulphur Creek suite (*e.g.*, Mortensen, 1990; Piercey *et al.*, 2006; Colpron *et al.*, 2016a,b).

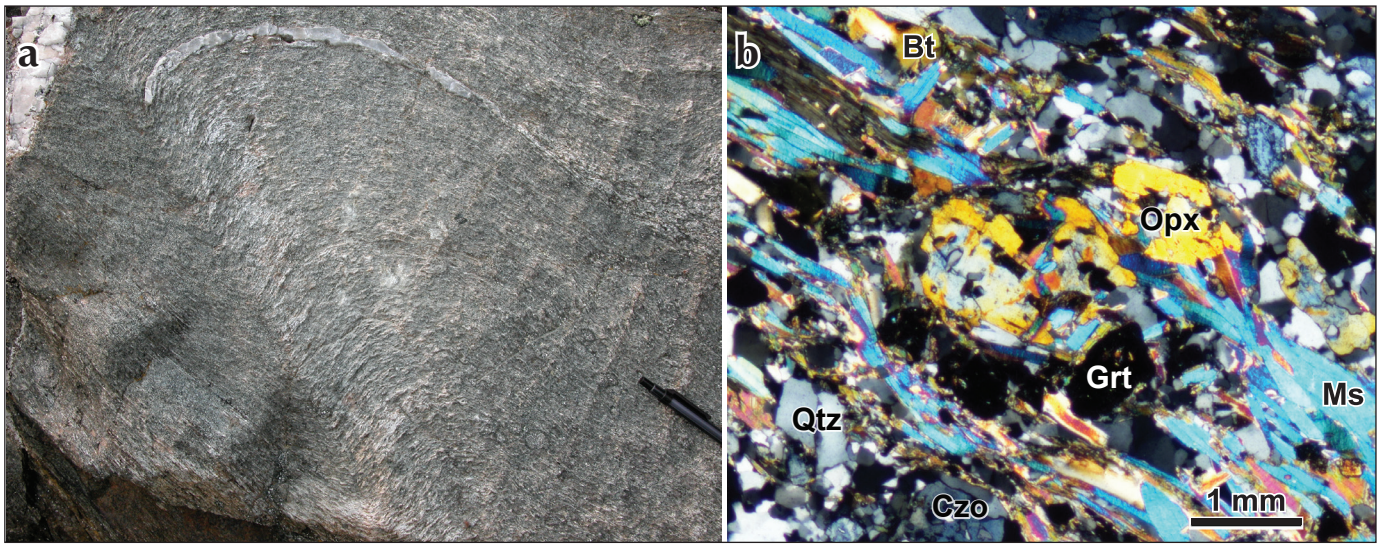

Figure 19. ***(a)*** *Outcrop of strongly foliated and folded metagranodiorite sampled for U-Pb geochronology (sample 04MC034-1; Table 4; Fig. 18c).* ***(b)*** *Photomicrograph (cross-polarized light) of penetratively deformed and metamorphosed muscovite-biotite-pyroxene metagranodiorite representative of geochronology sample 04MC034-1. Bt=biotite; Czo=clinozoisite; Grt=garnet; Ms=muscovite (phengite?); Opx=orthopyroxene (jadeite?); Qtz=quartz.*

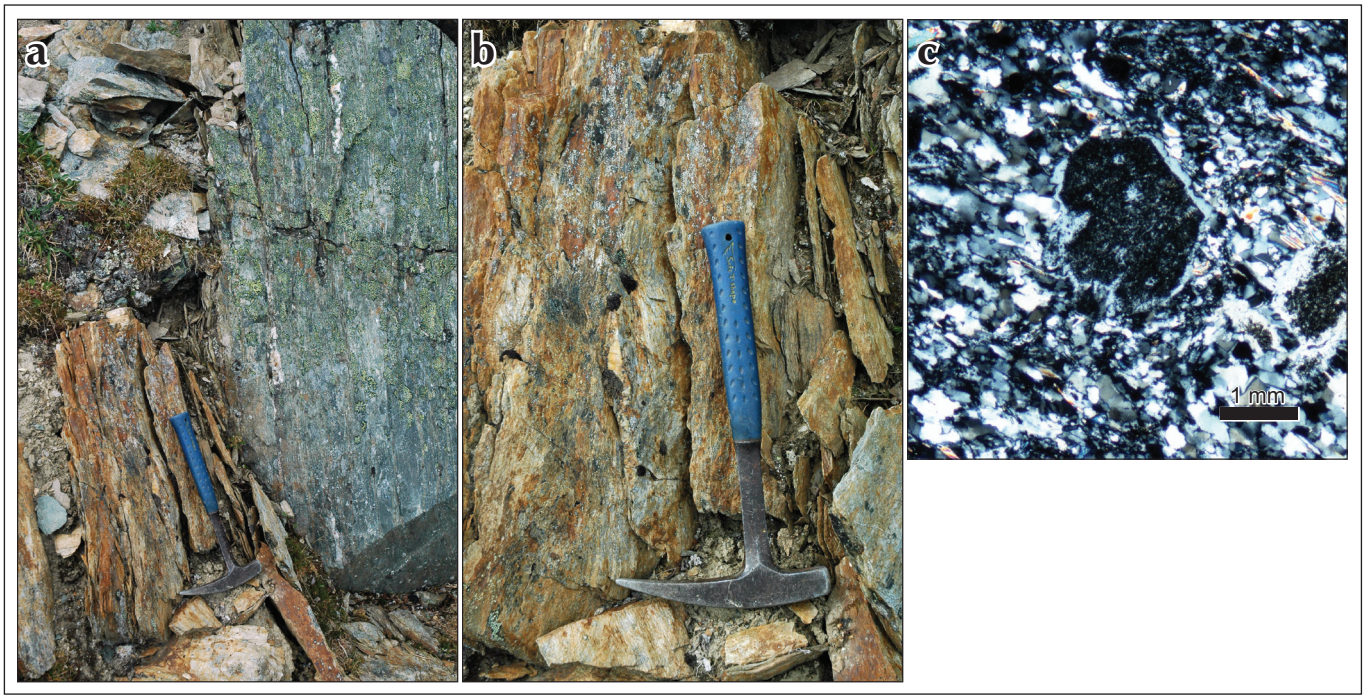

Figure 20. ***(a)*** *Felsic schist in contact with greenstone of the Mendocina succession (to right of hammer; locality 04MC101-3).* ***(b)*** *Closer view of felsic schist from locality 04MC101-3, dated at ca. 260 Ma (Fig. 18; Table 4).* ***(c)*** *Photomicrograph (cross-polarized light) of felsic plagioclase-muscovite schist containing a relict plagioclase phenocryst. Although the rock is penetratively deformed and metamorphosed, relict phenocrysts and concentric oscillatory zoning in zircon indicate an igneous origin. The schist is interpreted as a dike that intruded the Mendocina succession and was subsequently deformed and metamorphosed during a regional event.*

YT96-BS093 – DEFORMED MUSCOVITE-BIOTITE LEUCOCRATIC PEGMATITE

Foliated, lineated, boudinaged and folded, muscovite and biotite-bearing, leucocratic granite and pegmatite lenses, sills and concordant layers range in thickness from a few centimetres to 5 m (Fig. 21a,b). They intruded garnet amphibolite of the Snowcap assemblage east of the large Mississippian pluton (Fig. 2). The contacts and internal foliation in the leucogranite are generally concordant with the penetrative transposition foliation (S_T) in chlorite, biotite or muscovite-chlorite-feldspar schist of the Snowcap assemblage; however, leucogranite contacts locally crosscut S_T (Fig. 21c), suggesting emplacement during or after deformation.

Zircon crystals are igneous on the basis of euhedral bipyramidal morphology and high uranium content. Zircon tips were chosen for analysis to avoid cores with inherited Pb. Three fractions of single abraded tips were analyzed (Table 4; Fig. 18e) and are 1.9% to 4.8% discordant due to recent Pb loss. The date of 243.0±1.5 Ma is based on the age of upper intercept of a discordia chord through the origin of the three discordant fractions (MSWD 0.76). The age is interpreted as the crystallization age of the leucogranite and pegmatite.

DISCUSSION

The Snowcap assemblage has been defined and described by Colpron *et al.* (2006, 2016b; Piercey and Colpron, 2009) and is interpreted as the 'basement' to the Yukon-Tanana terrane, intruded by plutons of the Simpson Range suite. In the Livingstone Creek area, the lithological character of metasedimentary rocks in the Snowcap assemblage (Colpron, 2005a,b), the geochemical signatures of associated greenstone and amphibolite (Figs. 12-14), and intrusion by a *ca.* 351 Ma calc-alkaline metagranodiorite (MqSR, Figs. 2 and 18c) are all consistent with the regional character of the Snowcap assemblage.

On the basis of lithology and geochemistry, the calc-alkaline metavolcaniclastic and metasedimentary rocks of the Livingstone Creek succession correlate well with Devonian-Mississippian arc rocks of the Finlayson assemblage elsewhere in Yukon-Tanana terrane (*e.g.*, Little Kalzas formation, Colpron, 2001; Colpron *et al.*, 2002, 2006). However, their age in the Livingstone Creek area is not well constrained. East of May Creek (Fig. 2), the metavolcaniclastic rocks are crosscut by a penetratively foliated metatonalite inferred to be an apophysis from the large Early Mississippian pluton to the north; this provides a minimum age of *ca.* 351 Ma for the Livingstone Creek succession.

In the northeast part of the Livingstone Creek map area, micaceous quartzite, quartzite and marble of the Last Peak succession are interpreted to have been intruded by a *ca.* 358 Ma augen granite orthogneiss (DMgG, Figs. 2 and 18a,b; Gallagher, 1999; Colpron, 2005a). Although the lithological character of the Last Peak metasedimentary rocks is similar to and could perhaps be correlated with the Snowcap assemblage (*i.e.*, pre-Late Devonian), it is more likely that they are part of the Finlayson assemblage. The westward transition to graphitic phyllite and quartzite (DMFbp, Figs. 2 and 6a) is more typical of basinal facies of the Finlayson assemblage supporting a correlation with this younger, Late Devonian–Early Mississippian part of the terrane (Colpron *et al.*, 2006, 2016b). Graphitic lithology becomes more extensive east of the d'Abbadie fault (Figs. 2 and 11) where it can be traced more than 50 km southward to Quiet Lake, and farther south to Swift River (Colpron *et al.*, 2016b). This belt of graphitic rocks is interpreted as a basinal (back-arc?) environment within the Finlayson assemblage (Colpron *et al.*, 2006).

The Mendocina greenstone, with predominantly igneous protoliths, stands in contrast with the metasedimentary rocks of the Snowcap and Last Peak successions, to the west and east (Fig. 2). An oceanic environment is indicated for the Mendocina succession by the association of NMORB with ultramafic rocks and minor graphitic phyllite (Colpron, 2005a,b). Colpron (2005b) suggested correlation with mafic and ultramafic rocks of the Upper Devonian Fire Lake formation in the Finlayson Lake district (Fig. 1; Piercey *et al.*, 2004; Murphy *et al.*, 2006; older part of Finlayson assemblage, Colpron *et al.*, 2006). The Fire Lake formation includes a wide range of geochemical signatures including primitive arc and arc-rift rocks (including boninite), in addition to NMORB (Piercey *et al.*, 2001, 2004). Alternatively, the Mendocina succession could correlate with oceanic rocks of the Lower Mississippian to Lower Permian Slide Mountain terrane (*e.g.*, Colpron *et al.*, 2006). However, rocks of the Slide Mountain terrane are typically less deformed and metamorphosed than the Mendocina succession, and occur along the eastern edge of Yukon-Tanana terrane, not within it. Another interpretation is that the Mendocina succession represents an intra-Yukon-Tanana oceanic tract. The age of the Mendocina greenstone in the Livingstone Creek area is constrained by a *ca.* 260 Ma felsic dike that crosscuts greenstone and black phyllite (Figs. 2, 18d and 20).

Figure 21. *YT96-BS093 geochronology locale. Outcrop photos* ***(a)****,* ***(b)*** *and* ***(c)*** *show deformed muscovite and biotite-bearing leucogranite and pegmatite hosted in muscovite-chlorite-feldspar schist. The leucogranite and pegmatite locally crosscut the foliation in the schist, but are themselves foliated and folded. Hammer for scale in* ***(a)*** *is highlighted by white circle.*

The Mendocina greenstone projects northwest to the Big Salmon River where it was metamorphosed to eclogite facies conditions at 269 Ma (Fig. 4). This further constrains the minimum age of the Mendocina succession. Occurrences of sodic amphibole (Fig. 15) and phengitic mica in the Livingstone Creek area suggest that it was also subjected to high-pressure conditions (Hansen, 1992). This is also supported by the mineral assemblage in metagranodiorite sample 04MC034-1 (Fig. 19b; jadeite? + phengite? + quartz + biotite + garnet + clinozoisite), which is indicative of high-pressure (eclogite, blueschist) conditions (*e.g.*, Yardley, 1989; Proyer, 2003). This would imply that much of the Livingstone Creek area was subject to eclogite facies metamorphism, probably in mid-Permian. However, our observations are only qualitative and need to be confirmed quantitatively before reaching a definitive conclusion. This would be consistent with interpretation that much of the St. Cyr area to the south (Fig. 1) was metamorphosed at eclogite facies conditions in Permian time (Petrie *et al.*, 2015, 2016).

Development of the regional transposition foliation probably began with (or before) dynamic high-pressure metamorphism at *ca.* 269 Ma. The *ca.* 260 Ma felsic dike that crosscut the Mendocina assemblage has not been subjected to the same deformation and metamorphism as older rocks, as indicated by preservation of plagioclase phenocrysts (Fig. 20c). Similar (coeval?) granitic dikes

near the headwaters of Cottoneva and Little Violet creeks are described by Colpron (2005b) as weakly foliated and boudinaged, possibly syntectonic with respect to the development of the dominant foliation. Syn to post-deformation, two-mica granite and pegmatite dated at *ca.* 243 Ma south of Livingstone Creek (YT96-BS093, Figs. 2, 18e and 21), provide a minimum age on development of the regional transposition foliation. These constraints are consistent with the concept of a Permo-Triassic Klondike orogeny in the Yukon-Tanana terrane (Beranek and Mortensen, 2011). The end of ductile deformation in the centre of the Livingstone Creek area is ultimately constrained by Early Jurassic (*ca.* 195-190 Ma) $^{40}Ar/^{39}Ar$ mica cooling ages (Colpron, 2005a).

MINERAL POTENTIAL

The Livingstone Creek area is not only prospective for gold but also for a range of mineralization types including polymetallic veins, syngenetic base metals, skarn, and altered ultramafic rocks (*e.g.*, nephrite jade).

Placer gold has been extracted from at least eight creeks in the Livingstone district. Most of these are narrow, deeply incised valleys that are generally less than 3 km in length, and are oriented east-west (Fig. 2). The coarse gold is commonly associated with magnetite, garnet, galena, pyrite, hematite, cinnabar and cassiterite, which is an association of minerals that could indicate an intrusion-related or epithermal source for the gold (Fig. 22). Common occurrence of coarse magnetite in the placer deposits could also indicate a skarn origin. The coarse nature of the gold in the Livingstone placer deposits suggests local derivation from the east, toward the large Early Mississippian pluton that intruded the Snowcap assemblage (Fig. 2).

Magnetic anomaly B (Fig. 9) at the headwaters of the placer creeks may point to a source for the magnetite, and possibly the gold. Smaller anomalies to the west, toward the South Big Salmon River, parallel lineament B and may represent other magnetite-bearing structures. The electromagnetic conductor along the west flank of the Mississippian pluton (#1 on Fig. 11) may be related to magnetic lineament B (Fig. 9) and represents a target worth further investigation.

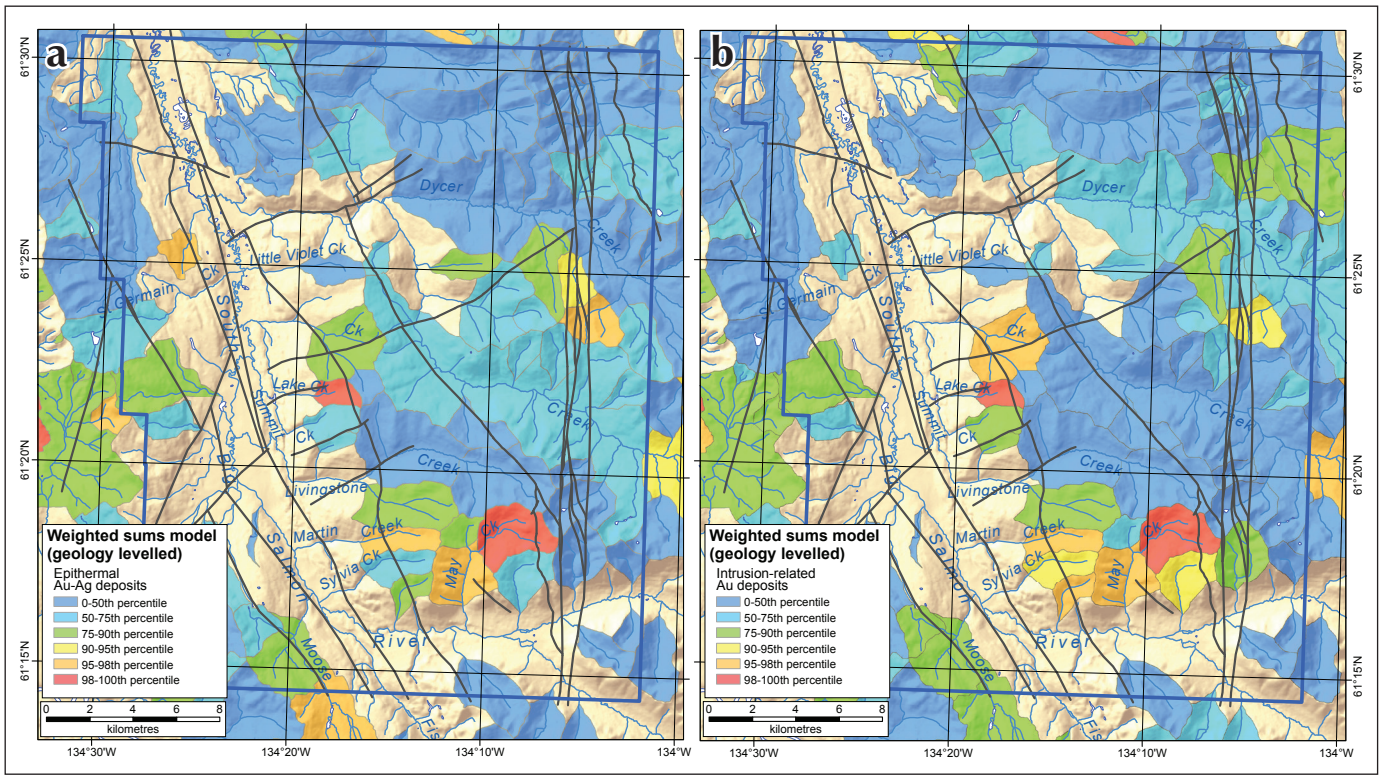

Figure 22. *Weighted sum models of regional stream sediment geochemical data leveled by mapped geology for:* ***(a)*** *epithermal Au-Ag deposits; and* ***(b)*** *intrusion-related Au deposits (from Mackie et al., 2016).*

Early exploration efforts identified occurrences of quartz-carbonate-sulphide veins between Sylvia and Lake creeks, some with visible gold (Fig. 23; Yukon MINFILE, 2016 – 105E 001, 105E 042, 105E 053). The veins are generally concordant with the dominant north to northwest-striking foliation, and locally offset by north to northeast-striking brittle faults. Stroink and Friedrich (1992) noted Au enrichment near the faults, and suggested that placer gold originated from the veins based on chemistry, mineralogy and fluid inclusions.

Having noted common, but subtle northeast-trending lineaments in the tilt derivative of the magnetic intensity data (Fig. 10), and their local coincidence with mapped brittle faults, we identified magnetic lineaments in the N020 direction (± approximately 20°) using the 020/200 bi-directionally gridded image in order to highlight potential northeast-striking structures (Fig. 23). We also identify northeast-trending lineaments from 020/200 bi-directional gridding of the early conductivity data (Appendix 1; Fig. 23). Although this analysis is not rigorous, it is nonetheless remarkable that most northeast-lineaments cluster in the area between Sylvia and Little Violet creeks, in the vicinity of known placer operations.

The association of primitive greenstone of the Mendocina succession with graphitic phyllite of the Last Peak succession is prospective for volcanogenic massive sulphide (VMS) style of mineralization (Figs. 2 and 24). The strong conductivity attributed to the graphitic lithology northeast of Mendocina Creek could mask VMS-style sulphide deposits (Fig. 11). A coincident magnetic anomaly (E on Figs. 9 and 10) represents a potential exploration target. A small greenstone lens in graphitic schist, that contains disseminated sulphide and malachite, is mapped within this anomaly and returned anomalous Cu-Zn values (05MC011-1, Table 5).

The strong linear conductor north of Dycer Creek (#2 on Fig. 11) is related to a sheared greenstone unit in the Last Peak succession (DMFv, Figs. 2 and 6c). Disseminated pyrrhotite was noted along the contact between the greenstone and marble (Figs. 6d and 25), but returned only slightly anomalous Cu values (05MC083-1, Table 5).

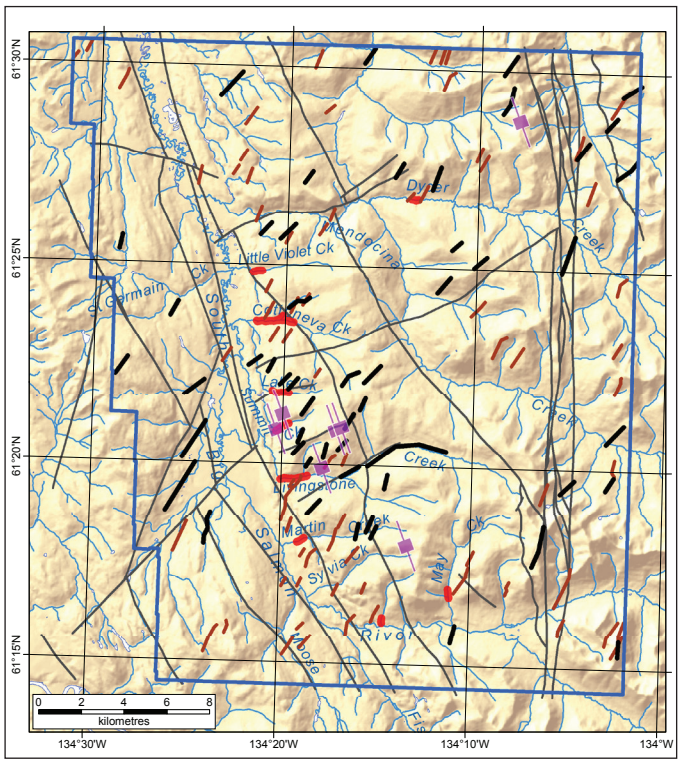

Figure 23. *Northeast-trending lineaments identified in magnetic (Fig. 10, Appendix 1a; black lines) and early conductivity (Appendix 1b; brown lines) data are plotted over shaded relief along with known quartz-carbonate-sulphide veins (purple squares) and placer mining operations (red lines). Lineament shapefiles are provided in Appendix 1c.*

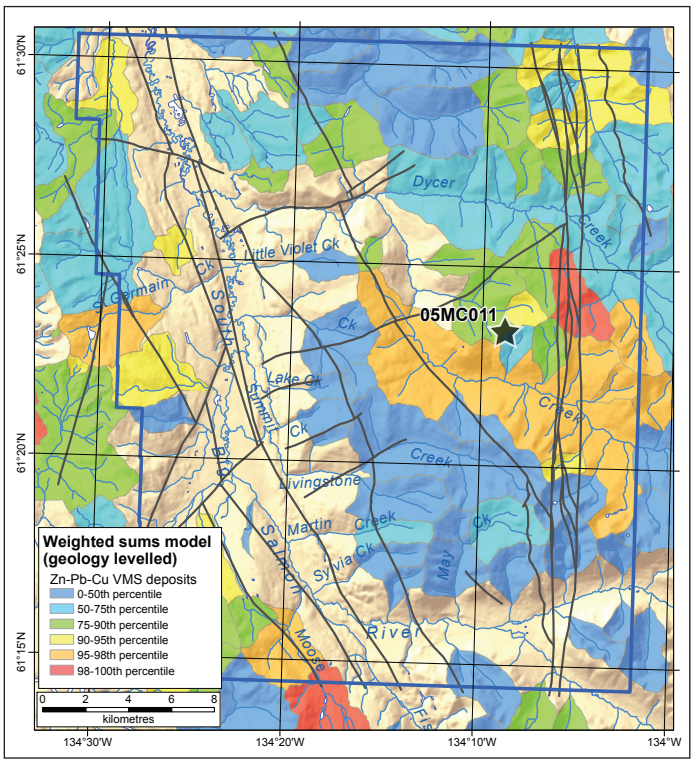

Figure 24. *Weighted sum model of regional stream sediment geochemical data leveled by mapped geology for Zn-Pb-Cu VMS deposits (from Mackie et al., 2016). Star indicates location of assay sample 05MC011, listed in Table 5.*

The eastern flank of the same conductor (2 on Fig. 11) coincides with a series of quartz veins locally rich in galena (Fig. 26). Three grab samples from these veins returned 2.03-7.78% Cu and 52-108 g/t Ag (05MC085 1-3, Table 5), and the potential for other similar polymetallic veins is good (greater than 90th percentile) along the d'Abbadie fault corridor based on enhanced interpretation of regional geochemical data (Fig. 27).

East of the d'Abbadie fault, the main known mineral occurrences are W-Cu skarn associated with the *ca.* 112 Ma Dycer stock exposed beyond the limit of the map area (Fig. 2; Minfile 105E 031, 105E 065, Fig. 11; Gallagher, 1999; Westberg, 2009). Four grab samples from skarn mineralization returned anomalous Cu-Pb-W values (05MC101, 05MC105, Table 5).

Finally, the new aeromagnetic survey could help locate magnetite-rich placer deposits in the area. For example, a strong magnetic high originates from the ultramafic massif at the headwaters of Livingstone Creek (Figs. 2 and 5) and generally follows its valley. However, the modern creek is locally offset from the magnetic anomaly, thereby suggesting that paleo-channels may be buried along the sides of the valley (Fig. 28).

Figure 25. *Close-up view of pyrrhotite-bearing greenstone in contact with marble, Last Peak succession (locality 05MC083-1, Fig. 11; Table 5).*

ACKNOWLEDGEMENTS

Warner Miles (GSC) provided guidance in design of the geophysical survey, oversaw data acquisition and quality control, and arranged for production of the open file releases. Discussions with Scott Casselman and Jeff Bond (YGS) helped steer interpretation of the mineral and placer potential of the area. Steve Israel commented on an earlier version of the manuscript. Finally, thanks to Leyla Weston for editing this paper.

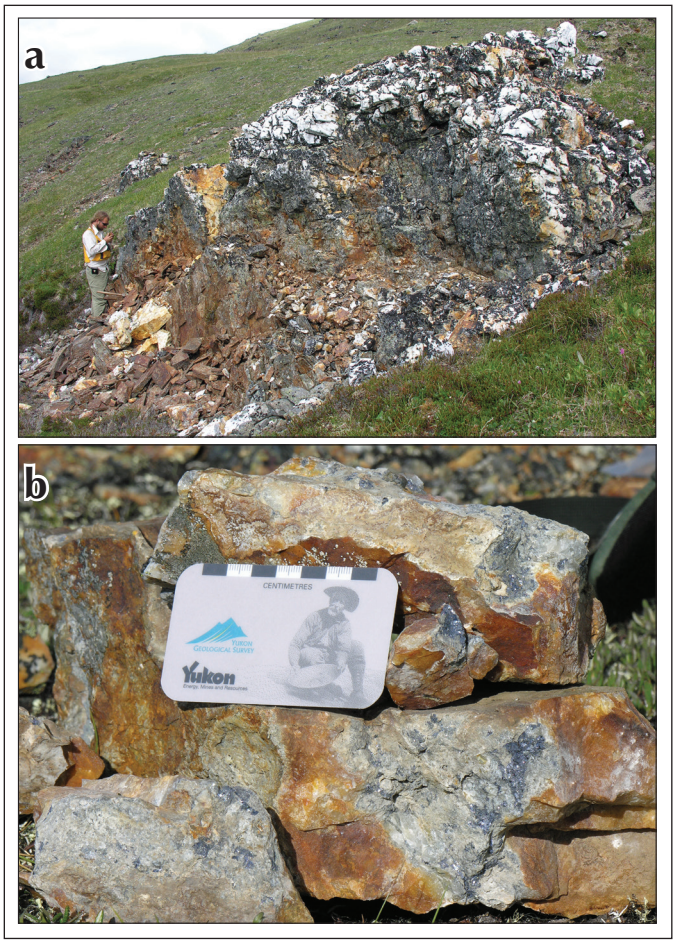

Figure 26. ***(a)*** *Quartz-galena vein at the RK occurrence (Yukon MINFILE 105E 064; Fig. 11; 05MC085-3, Table 5).* ***(b)*** *Close-up of galena mineralization (05MC085-2, Table 5).*

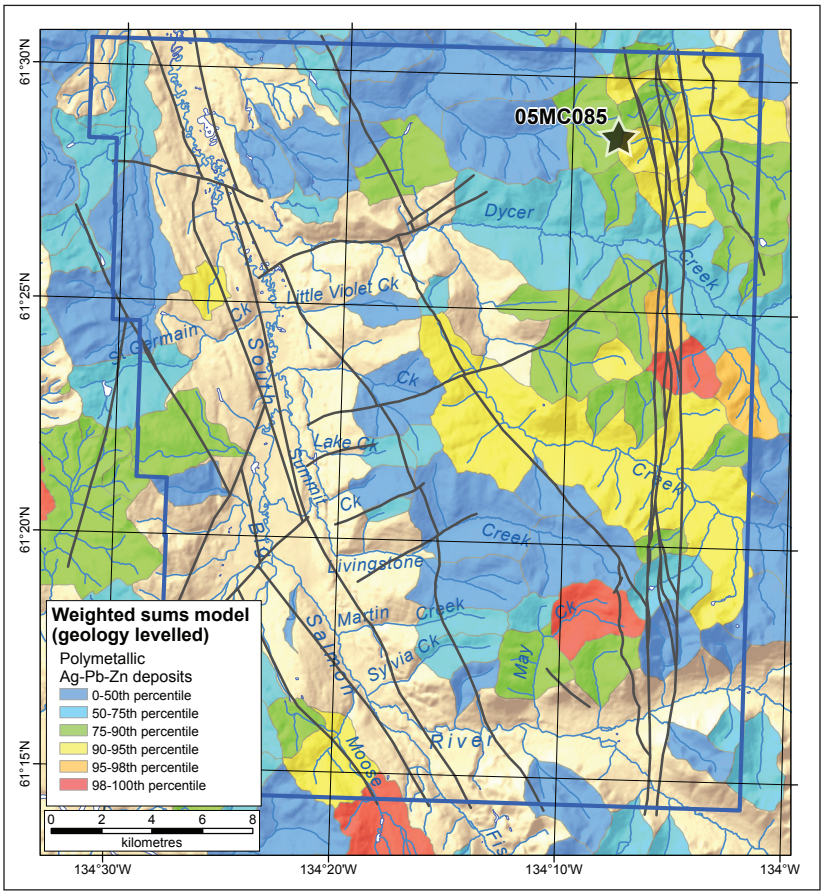

Figure 27. *Weighted sum model of regional stream sediment geochemical data leveled by mapped geology for polymetallic vein (Ag-Pb-Zn) deposits (from Mackie et al., 2016). Star indicates location of assay sample 05MC085, listed in Table 5.*

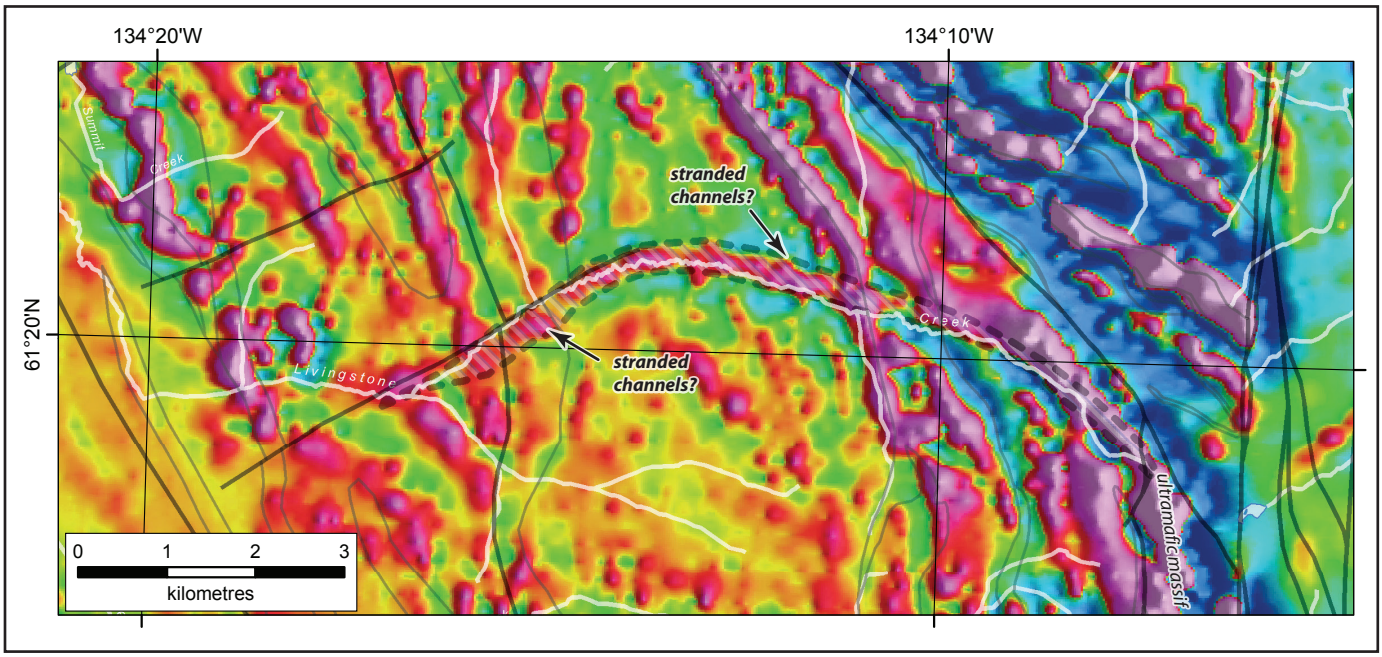

Figure 28. *The magnetic high following the outline of the Livingstone Creek valley (hatched) is ascribed to magnetite eroded from the ultramafic massif at the headwaters of the creek. Note that this magnetic train locally deviates from the modern stream course, suggesting possible buried channels on the valley flanks. First vertical derivative of the magnetic field from Boulanger et al. (2016b).*

Table 1. *Geochemical analyses of metavolcanic rocks from the Livingstone Creek area. The excel file for Table 1 is available at http://data.geology.gov.yk.ca/.*

SAMPLE	02MC124	04MC108	04MC115	04MC146	04MC056	04MC058	04MC059	04MC060
	Snowcap assemblage				Livingstone Creek succession			
Map unit	PDSv	PDSv	PDSv	PDSv	DMFi	DMFi	DMFi	DMFi
Lithology	amphibolite	mafic schist	metagabbro	metagabbro	chl schist	felsic schist	felsic schist	felsic schist
Affinity	MORB	CA	OIB	OIB	CA	CA	CA	CA
Latitude	61.315	61.392	61.368	61.297	61.302	61.300	61.300	61.298
Longitude	-134.169	-134.264	-134.257	-134.266	-134.134	-134.129	-134.150	-134.152
SiO_2	49.33	52.87	44.99	49.03	50.85	66.21	66.15	66.96
TiO_2	1.76	0.70	2.32	1.06	0.83	0.68	0.68	0.51
Al_2O_3	13.56	18.23	11.12	12.69	17.01	15.23	15.24	14.37
Fe_2O_3	13.27	8.79	11.17	10.33	8.87	5.39	5.85	5.07
MnO	0.273	0.134	0.181	0.154	0.136	0.092	0.093	0.098
MgO	7.33	5.44	8.57	8.65	5.06	2.01	1.99	0.54
CaO	8.98	6.90	12.83	10.96	6.04	2.27	2.23	1.22
Na_2O	1.88	4.29	2.67	2.13	5.31	2.83	2.89	5.38
K_2O	1.4	0.63	0.40	1.78	1.34	3.09	3.10	3.12
P_2O_5	0.15	0.25	0.61	0.18	0.20	0.14	0.14	0.18
Cr_2O_3	-	0.01	0.10	0.06	0.01	0.01	-0.01	-0.01
LOI	2.27	1.92	5.40	3.41	4.52	2.16	1.92	1.88
TOTAL	100.23	100.16	100.36	100.43	100.18	100.11	100.27	99.32
Cr	97	43	588	430	79	77	56	-20
Ni	58	27	118	329	116	-20	-20	-20
Co	42	22	33	48	30	9	7	3
Sc	-	26.7	26.0	28.7	26.2	10.3	10.7	10.5
V	347	181	173	185	241	47	44	6
Cu	10	-10	59	-10	109	22	26	-10
Pb	6	7	-5	6	8	27	19	33
Zn	176	72	93	77	68	80	62	83
Rb	26	15	9	53	43	87	88	60
Cs	0.5	0.1	0.2	1.0	5.3	7.4	7.1	0.8
Ba	1,000	138	279	1,150	549	3,070	3,170	3,050
Sr	313	466	837	417	251	733	739	102
Ga	18	21	18	17	19	19	19	20
Ta	0.16	0.38	1.99	0.95	0.27	0.84	0.84	0.99
Nb	4.3	7.0	31.6	18.4	6.0	12.9	13.1	15.5
Hf	2.8	1.5	4.0	1.6	2.5	5.3	5.3	6.3
Zr	108	58	161	59	93	201	208	240
Y	38.8	13.1	29.2	17.0	16.5	31.3	30.7	38.4
Th	0.22	2.67	3.35	1.70	4.77	9.46	9.40	12.7
U	0.16	0.71	0.78	0.37	2.08	3.10	3.07	4.00
La	4.37	14.3	48.1	15.8	17.3	31.7	31.9	41.2
Ce	12.4	28.9	97.1	30.0	34.6	62.0	62.5	81.6
Pr	1.97	3.36	11.6	3.41	4.10	7.36	7.39	9.48
Nd	11	13.4	47.1	14.1	16.6	27.7	28.0	35.9
Sm	3.8	2.73	10.1	3.24	3.61	6.05	6.00	7.56
Eu	1.48	1.08	3.24	1.19	1.17	1.36	1.38	1.72
Gd	5	2.55	9.20	3.68	3.47	5.52	5.67	6.96
Tb	1.01	0.42	1.34	0.61	0.55	0.93	0.97	1.17
Dy	6.71	2.42	6.44	3.43	3.02	5.34	5.46	6.56
Ho	1.35	0.47	1.00	0.62	0.61	1.05	1.05	1.32
Er	4.21	1.36	2.44	1.66	1.84	3.23	3.23	4.16
Tm	0.642	0.203	0.307	0.227	0.265	0.477	0.471	0.628
Yb	3.92	1.40	1.70	1.33	1.62	3.01	3.08	4.04
Lu	0.571	0.220	0.225	0.170	0.241	0.438	0.441	0.607

Table 1 continued.

SAMPLE	04MC065	04MC072	04MC073	04MC077	04MC080-2 (1)	04MC080-2 (2)	04MC152	05MC018
	Mendocina succession							
Map unit	DMFv	DMFv	DMFv	DMFv	DMFv	DMFv	DMFv	DMFv
Lithology	metagabbro	greenstone	greenstone	greenstone	greenstone	greenstone	greenstone	greenstone
Affinity								
Latitude	61.319	61.320	61.326	61.334	61.345	61.345	61.337	61.383
Longitude	-134.128	-134.112	-134.109	-134.114	-134.139	-134.139	-134.115	-134.192
SiO_2	46.22	48.38	55.37	49.61	48.33	48.40	45.43	48.33
TiO_2	1.85	2.03	1.50	2.41	2.28	2.28	1.82	1.65
Al_2O_3	15.01	13.51	12.59	12.40	13.53	13.52	14.36	14.89
Fe_2O_3	9.12	12.68	11.41	14.19	14.02	14.04	13.07	11.48
MnO	0.130	0.210	0.191	0.217	0.216	0.217	0.218	0.182
MgO	4.94	6.61	6.61	6.88	6.60	6.59	9.81	7.45
CaO	14.07	9.43	8.21	7.99	10.41	10.38	9.17	9.22
Na_2O	3.71	3.79	3.23	4.24	3.30	3.30	2.54	3.55
K_2O	0.59	0.22	0.20	0.17	0.59	0.59	0.16	0.36
P_2O_5	0.23	0.20	0.15	0.24	0.23	0.23	0.16	0.17
Cr_2O_3	0.04	0.03	0.02	0.02	0.03	0.03	0.04	0.02
LOI	4.42	2.73	0.58	2.11	0.93	0.93	3.19	2.79
TOTAL	100.33	99.82	100.06	100.47	100.46	100.51	99.97	100.1
Cr	212	239	87	152	178	184	258	190
Ni	84	74	53	74	70	73	68	100
Co	34	40	41	43	42	44	51	50
Sc	33.5	34.8	33.2	37.2	38.3	-	44.4	29.7
V	271	391	269	412	388	405	316	328
Cu	-10	64	-10	33	20	21	13	100
Pb	-5	-5	-5	-5	-5	-5	-5	< 5
Zn	65	102	101	120	100	101	156	90
Rb	12	3	1		14	15	1	14
Cs	0.8	0.2	0.2	-0.1	0.8	0.8	-0.1	0.5
Ba	290	106	47	9	168	172	33	51
Sr	301	194	103	86	130	135	99	102
Ga	17	19	17	19	19	19	22	18
Ta	0.87	0.25	0.45	0.25	0.27	0.27	0.22	0.19
Nb	13.5	5.0	8.3	4.9	4.7	4.9	4.8	3.7
Hf	3.5	3.7	2.6	4.2	4.2	4.2	3.1	2.9
Zr	135	138	99	151	145	158	104	109
Y	30.0	47.1	30.7	52.0	49.6	51.6	39.6	37.3
Th	1.09	0.29	0.60	0.30	0.31	0.31	0.28	0.26
U	0.49	0.10	0.26	0.11	0.12	0.12	0.11	0.11
La	11.5	5.53	8.28	6.05	6.30	6.06	4.29	4.36
Ce	26.7	16.2	18.7	18.3	18.8	17.9	13.3	12.7
Pr	3.60	2.64	2.64	2.95	3.00	2.84	2.17	2.12
Nd	16.0	14.8	12.8	16.3	16.2	15.7	12.7	11.7
Sm	4.49	4.79	3.85	5.34	5.29	4.99	4.26	3.81
Eu	1.61	1.75	1.40	1.87	1.85	1.81	1.70	1.47
Gd	5.42	6.44	4.85	7.24	7.19	7.01	5.91	4.89
Tb	0.95	1.23	0.88	1.36	1.33	1.31	1.11	0.93
Dy	5.55	7.84	5.38	8.82	8.48	8.47	7.11	6.07
Ho	1.11	1.66	1.09	1.87	1.84	1.80	1.51	1.22
Er	3.28	5.03	3.28	5.74	5.67	5.48	4.58	3.7
Tm	0.470	0.738	0.473	0.848	0.830	0.824	0.667	0.57
Yb	2.86	4.64	2.96	5.17	5.25	5.21	4.12	3.54
Lu	0.402	0.671	0.434	0.755	0.758	0.753	0.592	0.507

Table 1 continued.

SAMPLE	05MC042	05MC075	05MC086-2	04MC136	05MC096	05MC189	05MC192	05MC217
	Last Peak succession			Klinkit assemblage				
Map unit	DMFs	DMFs	DMFs	CKv	CKv	CKv	CKv	CKv
Lithology	chl schist	chl schist	amphibolite	chl phyllite	gabbro dike	chl phyllite	chl phyllite	bt schist
Affinity								
Latitude	61.414	61.470	61.479	61.387	61.432	61.370	61.364	61.371
Longitude	-134.182	-134.134	-134.130	-134.060	-134.035	-134.031	-134.034	-134.057
SiO_2	57.75	46.75	46.87	42.70	47.78	47.96	47.64	46.65
TiO_2	0.92	1.43	1.84	1.73	1.98	1.87	2.03	1.9
Al_2O_3	15.75	16.23	15.06	14.19	14.42	14.5	15.34	13.48
Fe_2O_3	9.93	10.92	11.54	9.14	13.19	11.61	11.71	13.31
MnO	0.138	0.157	0.161	0.131	0.174	0.178	0.155	0.183
MgO	5.19	7.5	7.85	6.17	7.06	7.32	6.88	5.8
CaO	2.9	12.29	11.54	13.06	10.02	7.28	7.22	7.06
Na_2O	3.76	2.44	2.75	2.93	2.28	3.9	3.11	1.99
K_2O	0.42	0.23	0.31	0.11	0.38	1.01	2.08	3.49
P_2O_5	0.09	0.12	0.18	0.38	0.22	0.33	0.33	0.3
Cr_2O_3	< 0.01	0.05	0.04	0.05	0.03	0.01	0.02	< 0.01
LOI	3.29	1.19	0.92	8.61	1.96	3.17	2.46	4.83
TOTAL	100.1	99.31	99.06	99.20	99.5	99.14	98.98	98.98
Cr	< 20	380	280	267	230	50	120	< 20
Ni	< 20	120	110	137	50	30	60	30
Co	16	59	44	33	45	22	25	29
Sc	36.3	38.6	37.3	26.3	39.6	29.1	32.7	31.4
V	343	331	359	216	340	192	229	209
Cu	20	90	< 10	19	40	40	< 10	< 10
Pb	< 5	< 5	< 5	-5	< 5	< 5	< 5	6
Zn	< 30	80	60	63	80	< 30	60	60
Rb	10	4	4	3	6	16	43	125
Cs	0.4	0.6	2.2	-0.1	0.6	0.2	1.3	7.7
Ba	39	24	94	14	104	431	1620	3460
Sr	97	157	213	352	234	225	257	401
Ga	11	19	20	16	20	15	16	14
Ta	0.02	0.07	0.2	2.88	0.72	2.13	2.09	1.78
Nb	0.7	1.9	4.2	46.3	10.4	31.1	31.2	27.8
Hf	1.2	2.5	3.4	3.3	3.3	3.7	4.1	3.6
Zr	42	88	128	137	118	146	159	133
Y	20.8	34.6	42.1	23.6	35.3	26.8	31.7	32.4
Th	0.23	0.18	0.26	3.75	1.22	2.94	2.79	2.31
U	0.97	0.15	0.13	0.53	0.38	0.81	0.71	0.61
La	2.86	2.93	5	29.6	12.5	22.2	22.1	19.2
Ce	7.29	9.26	14.5	56.6	28.3	46.2	45.4	37.3
Pr	1.12	1.66	2.41	6.44	3.82	5.59	5.54	4.64
Nd	6.01	9.56	13.3	24.7	17.5	22.7	23.4	19.4
Sm	1.98	3.32	4.32	5.12	4.77	5.07	5.46	4.76
Eu	0.772	1.3	1.61	1.67	1.79	1.78	1.89	1.84
Gd	2.53	4.34	5.54	4.90	5.54	5.15	5.78	5.3
Tb	0.49	0.84	1.05	0.80	0.99	0.85	0.99	0.94
Dy	3.33	5.58	6.81	4.47	6.29	4.98	5.9	5.66
Ho	0.72	1.16	1.4	0.87	1.27	0.96	1.15	1.14
Er	2.19	3.51	4.28	2.47	3.78	2.81	3.34	3.45
Tm	0.343	0.519	0.653	0.344	0.559	0.41	0.496	0.507
Yb	2.21	3.28	4.11	2.08	3.51	2.49	3.08	3.11
Lu	0.337	0.483	0.596	0.305	0.504	0.36	0.448	0.456

NOTES:
Affinity, interpreted from geochemical data: CA - calc-alkaline; MORB - mid-ocean ridge basalt; OIB - ocean island basalt.
Geographic coordinates in decimal degrees, projection WGS84.
Analytical Method: Samples were prepared using a ceramic mill and analyzed for major, trace, and rare-earth elements (REE) at Activation Laboratories in Ancaster, Ontario, using the 4Lithores package.
Major element concentrations were determined by lithium metaborate/tetraborate fusion inductively coupled plasma (ICP).
Trace elements and REE were analyzed by inductively coupled plasma mass spectrometry (ICP-MS) at research detection limits.
Detailed methods and detection limits are given at: http://www.actlabs.com/page.aspx?page=517&app=226&cat1=549&tp=12&lk=no&menu=64.

Table 2. *Geochemical analyses of metaplutonic rocks from the Livingstone Creek area. The excel file for Table 2 is available at http://data.geology.gov.yk.ca/.*

SAMPLE	05MC121	04MC034	04MC041	04MC042	05MC047	05MC057	05MC023	05MC099	05MC103	05MC106
	Grass Lakes suite	Simpson Range plutonic suite								
Map unit	DMgG	MqSR	MqSR	MqSR	MqSR	MqSR	MqSR	MqSR	MqSR	MqSR
Lithology	augen granite	granodiorite	tonalite	tonalite	granodiorite	granodiorite	diorite	augen granite	granite	augen granite
Latitude	61.458	61.310	61.316	61.306	61.444	61.487	61.426	61.439	61.451	61.426
Longitude	-134.109	-134.200	-134.184	-134.205	-134.299	-134.359	-134.200	-134.026	-134.036	-134.015
SiO_2	47.78	67.14	62.85	68.46	72.78	60.64	52.74	71.12	64.14	71.17
TiO_2	0.25	0.32	0.54	0.29	0.32	0.38	0.48	0.48	1.07	0.56
Al_2O_3	19.53	15.32	15.49	15.18	13.38	17.35	18.87	14.08	18.23	13.99
Fe_2O_3	5.38	4.66	6.64	4.02	3.63	5.46	8.31	2.77	1.86	2.28
MnO	0.119	0.112	0.123	0.089	0.071	0.11	0.095	0.034	0.015	0.027
MgO	10.43	1.62	2.75	1.19	1.59	1.59	3.37	1.12	1.93	1.23
CaO	12.05	4.67	5.47	4.23	0.61	2	3.95	1.75	2.55	3.21
Na_2O	1.93	2.71	2.55	2.82	5.33	2.68	7.38	3.12	4.74	2.38
K_2O	0.67	2.05	1.75	2.10	1.28	7.82	0.29	3.62	4.09	3.27
P_2O_5	0.04	0.09	0.11	0.09	0.08	0.23	0.02	0.18	0.16	0.18
Cr_2O_3	0.03	-0.01	-0.01	-0.01	< 0.01	< 0.01	0.01	< 0.01	0.01	< 0.01
LOI	1	1.65	1.61	1.37	0.95	1.48	3.22	0.77	0.77	1.08
TOTAL	99.21	100.33	99.87	99.83	100	99.73	98.73	99.03	99.57	99.37
Cr	20	38	22	-20	< 20	40	80	40	90	30
Ni	< 20	-20	-20	-20	< 20	< 20	20	< 20	30	< 20
Co	5	9	14	6	3	11	22	5	4	3
Sc	8.9	11.5	19.4	7.49	7.9	7.5	34.2	7.1	13.6	7.8
V	28	74	147	45	21	65	231	33	79	30
Cu	< 10	-10	-10	-10	10	20	< 10	< 10	20	< 10
Pb	9	18	5	12	< 5	12	< 5	9	10	< 5
Zn	30	87	42	38	40	60	60	< 30	< 30	< 30
Rb	177	59	49	53	33	287	6	151	160	102
Cs	9.8	1.1	0.9	0.8	0.5	3.1	0.3	6.4	11.2	2.8
Ba	674	754	651	733	763	2360	75	657	738	566
Sr	145	280	202	260	69	456	235	158	292	112
Ga	17	15	15	14	17	18	17	21	22	17
Ta	1.22	0.65	0.52	0.61	0.68	0.71	< 0.01	1.39	1.73	1.26
Nb	14.1	10.1	7.8	7.8	9	10.4	0.5	13.7	23.2	14.3
Hf	5.4	2.0	2.9	2.2	4.8	3	1	4.8	8.1	5.7
Zr	201	68	99	78	187	128	32	178	283	213
Y	19.2	13.2	17.3	11.4	28.8	17.8	16.5	23.3	34.6	24.4
Th	14.2	6.47	6.78	6.39	5.09	14.2	0.15	14.1	15.4	14.7
U	2.4	1.68	1.18	2.23	1.33	2.88	0.06	4.31	2.06	2.87
La	32.8	17.0	20.8	16.7	6.39	54.4	1.96	38	35.4	50.4
Ce	69.3	31.2	36.5	30.9	13.3	81.5	4.46	75.6	83.3	95.2
Pr	7.63	3.13	3.84	3.16	1.61	11	0.8	8.91	8.56	10.7
Nd	27.8	11.2	14.2	10.8	6.6	38.5	4.3	32.2	31.5	39.7
Sm	5.42	2.26	2.95	1.98	1.61	6.54	1.54	6.35	6.39	7.52
Eu	1.04	0.714	0.769	0.666	0.398	2.02	0.728	1.2	1.16	1.42
Gd	4.19	2.10	2.85	1.82	2.12	5.27	2.04	5.09	5.63	5.97
Tb	0.67	0.38	0.48	0.30	0.56	0.68	0.41	0.81	1.04	0.9
Dy	3.52	2.25	2.90	1.75	4.17	3.26	2.74	4.08	5.84	4.46
Ho	0.65	0.45	0.62	0.36	0.93	0.57	0.57	0.74	1.13	0.81
Er	1.95	1.37	1.98	1.15	3.06	1.66	1.79	2.15	3.57	2.33
Tm	0.291	0.211	0.307	0.189	0.502	0.244	0.273	0.318	0.555	0.333
Yb	1.86	1.48	1.98	1.31	3.3	1.58	1.69	1.97	3.5	2.08
Lu	0.267	0.228	0.291	0.208	0.509	0.23	0.26	0.287	0.505	0.287

Table 2 continued.

SAMPLE	04MC080-1	04MC101-3	04MC104	05MC020	05MC005	05MC007	05MC014-2
	Permian intrusions (Sulphur Creek suite?)						
Map unit	PqS	PqS	PqS	PqS	PqS	PqS	PqS
Lithology	granite	felsic schist	granite	granite	tonalite	tonalite	qtz monzonite
Latitude	61.345	61.340	61.409	61.434	61.393	61.393	61.385
Longitude	-134.139	-134.119	-134.277	-134.211	-134.120	-134.130	-134.172
SiO_2	67.47	68.67	61.38	61.55	58.25	64.28	60.14
TiO_2	0.26	0.30	0.48	0.32	0.39	0.37	0.52
Al_2O_3	16.96	16.47	15.52	19.18	17.69	16.5	16.59
Fe_2O_3	2.14	2.57	6.30	3.5	4.62	3.79	5
MnO	0.052	0.054	0.100	0.071	0.122	0.105	0.102
MgO	0.76	2.72	2.27	0.66	1.62	1.54	1.64
CaO	3.08	2.17	2.60	6.53	6.32	4.58	4.1
Na_2O	7.45	2.93	2.06	4.21	3.16	3.65	2.96
K_2O	0.61	1.98	6.99	1.8	2.17	2.46	3.33
P_2O_5	0.18	0.08	0.24	0.13	0.19	0.32	0.26
Cr_2O_3	0.07	-0.01	0.01	0.01	< 0.01	0.01	< 0.01
LOI	0.83	2.47	2.32	2.2	5.18	2.41	5
TOTAL	99.87	100.40	100.27	100.2	99.7	100	99.63
Cr	-20	-20	52	30	20	40	< 20
Ni	34	-20	-20	< 20	< 20	< 20	< 20
Co	2	2	13	7	8	7	7
Sc	1.56	8.89	11.0	5.6	8.9	5.2	9
V	41	17	81	97	108	90	138
Cu	-10	-10	34	40	20	20	20
Pb	11	23	33	7	7	7	< 5
Zn	66	62	78	40	40	60	60
Rb	12	61	351	47	64	74	76
Cs	-0.1	1.1	7.0	0.5	1.4	1.7	1.6
Ba	726	3,950	2,110	1220	1110	1130	3490
Sr	797	266	366	1330	976	813	409
Ga	20	23	17	26	19	17	19
Ta	0.13	0.79	0.98	0.17	0.18	0.2	0.45
Nb	3.6	10.5	13.3	3.8	3	3.4	6
Hf	1.9	5.5	4.3	2.2	2.4	2.1	3.1
Zr	62	214	172	79	96	83	115
Y	1.7	27.6	18.2	6.1	16.9	9.4	18.9
Th	0.28	12.5	18.3	1.19	2.99	1.37	4.16
U	0.25	3.79	2.89	0.82	1.73	0.84	1.8
La	1.93	36.6	42.4	10	13.9	6.17	16.8
Ce	3.83	69.8	81.3	18.9	25.4	12.1	31.9
Pr	0.43	7.87	8.72	2.37	3.03	1.48	3.83
Nd	1.78	28.6	30.5	9.66	11.9	5.95	14.6
Sm	0.38	5.63	5.54	2.03	2.6	1.39	3.18
Eu	0.126	1.53	1.27	0.681	0.92	0.478	0.835
Gd	0.30	4.90	4.36	1.56	2.65	1.37	3.02
Tb	0.04	0.82	0.63	0.22	0.45	0.24	0.55
Dy	0.25	4.63	3.34	1.03	2.68	1.49	3.1
Ho	0.05	0.94	0.62	0.19	0.55	0.3	0.62
Er	0.15	2.88	1.83	0.55	1.74	0.93	1.93
Tm	0.023	0.420	0.271	0.082	0.283	0.149	0.314
Yb	0.15	2.77	1.82	0.55	1.87	1.04	2.03
Lu	0.023	0.395	0.268	0.082	0.288	0.166	0.3

NOTES:
Geographic coordinates in decimal degrees, projection WGS84.
Analytical Method: Samples were prepared using a ceramic mill and analyzed for major, trace, and rare-earth elements (REE) at Activation Laboratories in Ancaster, Ontario, using the 4Lithores package.
Major element concentrations were determined by lithium metaborate/tetraborate fusion inductively coupled plasma (ICP).
Trace elements and REE were analyzed by inductively coupled plasma mass spectrometry (ICP-MS) at research detection limits.
Detailed methods and detection limits are given at: http://www.actlabs.com/page.aspx?page=517&app=226&cat1=549&tp=12&lk=no&menu=64.

Table 3. *Radiogenic isotopic data for 5 samples of metavolcanic rocks from the Livingstone Creek area.*

Sample	04MC080-2 (1)	05MC018	05MC086-2	05MC189	05MC217
Map unit	Mendocina	Mendocina	Last Peak	Klinkit	Klinkit
Rock type	greenstone	greenstone	amphibolite	chloritic phyllite	chloritic phyllite
Affinity	NMORB	NMORB	NMORB	OIB	OIB
Inferred Age	360	360	360	350	350
$^{143}Nd/^{144}Nd$	0.513	0.513	0.513	0.513	0.513
$^{147}Sm/^{144}Nd$	0.198	0.197	0.196	0.135	0.148
εNd(0)	8.0	8.5	8.7	2.2	3.4
εNd(t)	4.2	4.8	4.7	1.5	2.0
TDM(Nd) (Ga)	NA	NA	NA	1.39	1.61
$^{176}Hf/^{177}Hf$	0.283	0.283	0.283	0.283	0.283
$^{176}Lu/^{177}Hf$	0.026	0.025	0.025	0.014	0.018
εHf(0)	10.3	11.6	11.9	2.1	5.3
εHf(t)	5.0	6.5	6.6	-0.4	1.9
TDM(Hf) (Ga)	1.29	0.93	0.89	1.14	1.13

Notes:
Affinity, interpreted from geochemical data: NMORB - normal mid-ocean ridge basalt; OIB - ocean island basalt.
See Table 1 for geochemical analyses and geographic coordinates for these samples.
Sm/Nd and Lu/Hf analytical methods are given in Appendix 2.
NA = not available.

Table 4. *U-Pb analytical data for metaplutonic rocks from the Livingstone Creek area.*

Fraction[a]	Wt. (ug)[b]	U (ppm)	Pb* (ppm)[c]	$^{206}Pb^{d}/^{204}Pb$	Pb (pg)[e]	^{208}Pb %	Th/U	$^{206}Pb^{f}/^{238}U$	$^{207}Pb^{f}/^{235}U$	$^{207}Pb^{f}/^{206}Pb$	$^{206}Pb/^{238}U$ Age (Ma)[g]	$^{207}Pb/^{235}U$ Age (Ma)[g]	Corr. Coeff.	$^{207}Pb/^{206}Pb$ Age (Ma)[g]	% Discord.
YT95-BS082. AUGEN GRANITE ORTHOGNEISS – DMgG (Map 105E/8; UTM 546150 E, 6818700 N, NAD 83)															
A	91	281	33	5181	34	11.2	0.493	0.10913±.12	1.8577±.13	0.12346±.04	667.7±1.5	1066.2±1.7	0.95	2006.0±1.5	70.1
B	134	373	40	6404	51	8.4	0.342	0.10332±.32	1.4049±.32	0.09861±.09	633.9±3.9	891.0±3.9	0.96	1598.1±3.3	63.3
E	10	676	36	1484	17	4.1	0.144	0.05708±.39	0.4225±.26	0.05369±.44	357.8±0.7	357.8±1.6	0.13	357.9±20	0.0
04MC034-1: CPX-BT META-GRANODIORITE – MqSR (Map 105E/8; UTM 542871 E, 6797626 N, NAD 83)															
B	22	198	11	489	33	7.7	0.280	0.05526±.18	0.4078±.59	0.05353±.51	346.7±1.2	347.3±3.5	0.56	351.2±23	1.3
E	22	344	19	1147	23	7.5	0.271	0.05537±.09	0.4088±.22	0.05355±.18	347.4±0.6	348.0±1.3	0.62	352.1±8.0	1.4
F	17	417	23	229	118	8.0	0.291	0.05476±.26	0.4039±1.3	0.05350±1.2	343.7±1.7	344.5±7.5	0.59	350.0±52	1.8
04MC101-3: FELSIC MS PL SCHIST – PqS - deformed and metamorphosed dike (Map 105E/8; UTM 547156 E, 6800964 N, NAD 83)															
A	12	482	25	602	34	9.1	0.331	0.04161±.19	0.2936±.63	0.05117±.53	262.8±1.0	261.4±2.9	0.55	248.7±25	-5.8
D	5	728	30	348	29	10.3	0.382	0.04133±.16	0.2925±.70	0.05133±.62	261.1±0.8	260.5±3.2	0.57	255.7±28	-2.1
YT96-BS093: DEFORMED LEUCOCRATIC MS PEGMATITE (Map 105E/8; UTM 544373 E, 6798327 N, NAD 83)															
A	8	6176	221	9200	12	5.4	0.188	0.03744±.23	0.26339±.22	0.05102±.11	237.0±1.1	237.4±0.9	0.88	241.6±5.2	1.9
B	10	3463	119	7177	12	1.6	0.051	0.03738±1.5	0.26302±.16	0.05104±.06	236.6±0.7	237.1±0.7	0.93	242.5±2.7	2.5
D	5	8860	306	6305	18	3.7	0.124	0.03637±1.3	0.25869±1.4	0.05107±.05	232.6±6.1	233.6±5.6	0.99	244.1±2.1	4.8

[a] s = single crystal, Letters(A-G) = zircon, M = monazite; [b] weighing error is 1 microgram; [c] radiogenic Pb; [d] Radiogenic Pb, corrected for spike and Pb fractionation of 0.09%±0.03%/amu; [e] total common Pb in analysis corrected for spike and fractionation; [f] corrected for Pb and U laboratory blank where 208/204:207/204:206/204 are 19.02:15.65:38.23, errors are 1 standard error of the mean in percent for ratios and 2 standard errors of the mean when expressed in Ma; and [g] corrected for common Pb and laboratory blank, errors are 2 standard errors of the mean in Ma.

***Table 5**. Assay results for grab samples collected in 2005 from the Livingstone Creek area.*

ELEMENT		05MC011-1	05MC083-1	05MC085-1	05MC085-2	05MC085-3	05MC101-3	05MC105-1	05MC105-2	05MC105-3
Rock		Chloritic Schist	Mafic schist	Qtz vein	Qtz vein	Qtz vein	Skarn	Skarn	Skarn	Skarn
Easting		545490	546505	546228	546228	546187	552213	552047	552047	552047
Northing		6806368	6815954	6816345	6816345	6816423	6812029	6812107	6812107	6812107
Mo	ppm	0.24	0.22	0.65	1.63	0.45	16.22	3.62	1.76	1.5
Cu	ppm	998.31	218.67	35.03	120.53	21.5	1883.65	369.7	1081.17	964.71
Pb	ppm	13.66	4.48	20300	77800	26300	594.64	400.06	68.87	30.22
Zn	ppm	3132.2	38.5	5.8	42.8	3.5	324	40.9	92.9	115.8
Ag	ppb	535	145	53530	108252	52468	2912	1315	1586	1456
Ni	ppm	8.9	28.9	5.2	6.5	2.8	7.8	61.5	31	28.9
Co	ppm	27.1	39.5	1.3	2.6	0.6	57.5	92.7	60	48.4
Mn	ppm	3257	174	24	812	32	1345	617	1163	1768
Fe	%	4.83	2.94	0.7	1.64	0.6	34.84	36.82	19.33	20.9
As	ppm	1.4	0.2	1.7	<.2	<.2	4.2	0.7	5.8	2
U	ppm	<.1	0.3	0.1	0.6	<.1	1.3	4.2	8.2	3.9
Au	ppm	15.7	1.4	<.1	<.1	<.1	<.1	<.1	<.1	<.1
Th	ppm	0.1	0.3	0.1	1.3	<.1	1.1	8.2	10.3	4.9
Sr	ppm	30.5	138.6	11	63	3	63	38	60	26
Cd	ppm	14.82	0.14	4.8	48.93	7.96	1.16	0.17	0.41	0.46
Sb	ppm	0.07	0.05	4.04	10.08	4.56	0.19	0.09	0.11	0.06
Bi	ppm	0.2	0.32	124.06	257.82	130.25	6.86	5.15	2.5	2.2
V	ppm	137	108	2	8	<1	3	36	44	57
Ca	%	1.01	2.46	0.07	2.14	0.05	6.94	4.05	7.01	8.76
P	%	0.032	0.128	0.003	0.23	0.019	0.016	0.043	0.09	0.054
La	ppm	1.1	1.9	1	5	<1	12	30	48	42
Cr	ppm	5.4	22.5	6	24	18	8	16	21	11
Mg	%	2.51	0.99	0.02	0.69	<.02	3.11	1.2	2.28	3.67
Ba	ppm	49.7	93	61	106	8	8	6	19	11
Ti	%	0.099	0.131	0.006	0.041	0.001	0.021	0.158	0.19	0.098
B	ppm	<1	1	-	-	-	-	-	-	-
Al	%	2.7	3.71	0.24	0.37	0.03	0.57	2.19	3.63	1.58
Na	%	0.021	0.307	0.112	0.126	0.019	0.045	0.561	1.286	0.421
K	%	0.04	0.38	0.09	0.11	<.02	0.07	0.05	0.08	0.09
W	ppm	<.1	0.1	0.1	0.3	<.1	0.2	0.6	50.1	2.7
Zr	ppm	0.8	0.4	2.1	7.6	2.5	3.1	7.7	22.2	11.4
Sn	ppm	0.1	0.4	0.9	2.5	1	1.7	2.5	10.3	3.2
Be	ppm	0.02	0.16	<1	<1	<1	2	10	30	16
Sc	ppm	7.2	5.1	0.2	1.3	<.1	0.3	4.6	4.5	17.4
S	%	0.14	0.91	0.48	1.38	0.63	>10	>10	7.86	>10
Y	ppm	3.99	7.98	0.4	19.9	1	2.2	21.3	53.2	34
Ce	ppm	3	4.6	1.13	9.65	0.26	18.66	62.8	97.77	81.36
Pr	ppm	-	-	0.1	1.2	<.1	1.8	6.4	10.3	8.6
Nd	ppm	-	-	0.4	5.8	0.1	5.8	23.4	40.4	34.3
Sm	ppm	-	-	0.1	1.7	<.1	0.8	4.8	8	7.2
Eu	ppm	-	-	<.1	0.8	<.1	0.7	0.5	1.2	1.2
Gd	ppm	-	-	0.1	2.4	0.1	0.7	3.8	7.2	6.4
Tb	ppm	-	-	<.1	0.5	<.1	0.1	0.7	1.3	1
Dy	ppm	-	-	0.1	3.8	0.2	0.5	4	8.3	6.6
Ho	ppm	-	-	<.1	0.8	<.1	0.1	0.6	1.5	1
Er	ppm	-	-	<.1	1.9	0.1	0.2	1.7	4.1	2.6
Tm	ppm	-	-	<.1	0.3	<.1	<.1	0.3	0.6	0.4

Table 5 continued.

ELEMENT		05MC011-1	05MC083-1	05MC085-1	05MC085-2	05MC085-3	05MC101-3	05MC105-1	05MC105-2	05MC105-3
Rock		Chloritic Schist	Mafic schist	Qtz vein	Qtz vein	Qtz vein	Skarn	Skarn	Skarn	Skarn
Easting		545490	546505	546228	546228	546187	552213	552047	552047	552047
Northing		6806368	6815954	6816345	6816345	6816423	6812029	6812107	6812107	6812107
Yb	ppm	-	-	0.1	1.7	0.1	0.1	1.7	5.2	3.4
Lu	ppm	-	-	<.1	0.2	<.1	<.1	0.3	0.7	0.6
Hf	ppm	0.03	0.02	0.08	0.22	0.06	0.11	0.28	1	0.38
Li	ppm	17.5	18.6	1.9	2.2	0.3	28	12.5	17.4	28.8
Rb	ppm	-	-	3.2	3.2	0.4	8.4	3.4	4.2	10
Ta	ppm	<.05	<.05	<.1	<.1	<.1	0.1	2.2	2.8	2.6
Nb	ppm	0.04	0.05	0.2	1.51	0.15	1.23	18.12	106.47	21.98
Cs	ppm	0.13	4.78	0.3	0.2	0.1	1.1	0.7	0.5	0.6
Ga	ppm	8.5	9.7	0.66	1.44	0.17	2.19	11.66	19.13	11.7
Hg	ppb	506	<5	-	-	-	-	-	-	-
Se	ppm	0.3	0.9	-	-	-	-	-	-	-
Te	ppm	0.11	0.02	-	-	-	-	-	-	-
Ge	ppm	0.1	0.2	-	-	-	-	-	-	-
Rb	ppm	1.9	18.3	-	-	-	-	-	-	-
In	ppm	0.05	0.02	-	-	-	-	-	-	-
Re	ppb	<1	<1	-	-	-	-	-	-	-
Be	ppm	0.1	0.9	-	-	-	-	-	-	-
Pd	ppb	<10	<10	-	-	-	-	-	-	-
Pt	ppb	<2	<2	-	-	-	-	-	-	-
		Trace of malachite + sphalerite	Hornfelsed; rusty talus with minor sulphides	Galena in Qtz vein; MINFILE 105E 064	Galena in Qtz vein; MINFILE 105E 064	Galena in Qtz vein. From 3 m wide vein ~80 m NW; MINFILE 105E 064	Po in Bt schist in contact aureole; MINFILE 105E 065	Semi-massive sulphide; MINFILE 105E 065	Semi-massive sulphide; MINFILE 105E 065	Semi-massive sulphide; MINFILE 105E 065

NOTES:
Samples analyzed at Acme Laboratories in Vancouver, BC.
Analysis: GROUP 1F30 - 30.00 GM SAMPLE LEACHED WITH 180 ML 2-2-2 HCL-HNO3-H2O AT 95 DEG. C FOR ONE HOUR, DILUTED TO 600 ML, ANALYZED BY ICP/ES & MS.
For galena samples (05MC085), Pb concentrations were determined by:
Analysis: GROUP 7AR - 1.000 GM SAMPLE, AQUA - REGIA (HCL-HNO3-H2O) DIGESTION TO 250 ML, ANALYZED BY ICP-ES.
Geographic coordinates are Universal Transverse Mercator (UTM) projection, zone 8, NAD83.

REFERENCES

Beranek, L.P. and Mortensen, J.K., 2011. The timing and provenance record of the Late Permian Klondike orogeny in northwestern Canada and arc-continent collision along western North America. Tectonics, vol. 30, p. TC5017, 10.1029/2010TC002849.

Bostock, H.S., 1957. The mining industry of Yukon, 1931. *In:* Yukon Territory – Selected field reports of the Geological Survey of Canada, 1898 to 1933, H.S. Bostock (ed.), Geological Survey of Canada, Memoir 284, p. 620-631.

Bostock, H.S. and Lees, E.J., 1938. Laberge map-area, Yukon. Geological Survey of Canada, 105E geological, 1:253,440, Memoir 217, 33 p.

Boulanger, O., Kiss, F. and Coyle, M., 2016a. Electromagnetic survey of the Livingstone Creek area, parts of NTS 105E/7, 8, 9 and 10. Yukon Geological Survey, Open File 2016-35, 1:20 000 scale; *also Geological Survey of Canada, Open File 8085*, <http://data.geology.gov.yk.ca/Reference/78483>.

Boulanger, O., Kiss, F. and Coyle, M., 2016b. Electromagnetic survey of the Livingstone Creek area, parts of NTS 105E/1 and 8. Yukon Geological Survey, Open File 2016-34, 1:20 000 scale; *also Geological Survey of Canada, Open File 8084*, <http://data.geology.gov.yk.ca/Reference/78483>.

Breitsprecher, K. and Mortensen, J.K. (eds.), 2004. Yukonage 2004: A database of isotopic age determinations for rock units from Yukon Territory, Canada. Yukon Geological Survey.

Cabanis, B. and Lecolle, M., 1989. Le diagramme La/10-Y/15-Nb/8; un outil pour la discrimination des séries volcaniques et la mise en évidence des processus de mélange et/ou de contamination crustale. Comptes Rendus de l'Académie des Sciences, Série 2, Mécanique, Physique, Chimie, Sciences de l'Univers, Sciences de la Terre, vol. 309, p. 2023-2029.

Carr, S.D., de Keijzer, M. and Gallagher, C. 1999. Progress report on U-Pb geochronology studies - Teslin zone and western Cassiar terrane, Yukon: Timing constraints on deformation and thermal history. *In:* Slave-Northern Cordillera Lithospheric Evolution (SNORCLE) Transect and Cordilleran Tectonic Workshop Meeting, F. Cook and P. Erdmer (eds.), Lithoprobe Report No. 69, p. 219-220.

Colpron, M., 2001. Geochemical characterization of Carboniferous volcanic successions from Yukon-Tanana terrane, Glenlyon map area (105L), central Yukon. *In:* Yukon Exploration and Geology 2000, D.S. Emond and L.H. Weston (eds.), Exploration and Geological Services Division, Yukon Region, Indian and Northern Affairs Canada, p. 111-136.

Colpron, M., 2005a. Geological map of Livingstone Creek area (NTS 105E/8), Yukon (1:50 000 scale). Yukon Geological Survey, Open File 2005-9.

Colpron, M., 2005b. Preliminary investigation of the bedrock geology of the Livingstone Creek area (NTS 105E/8), south-central Yukon. *In:* Yukon Exploration and Geology 2004, D.S. Emond, L.L. Lewis and G.D. Bradshaw (eds.), Yukon Geological Survey, p. 95-107.

Colpron, M., 2017. Revised geological map of the Livingstone Creek area (NTS 105E/8), Yukon. Yukon Geological Survey, Open File 2017-1, 1:50 000 scale.

Colpron, M. and Nelson, J.L., 2011. A digital atlas of terranes for the northern Cordillera. Yukon Geological Survey,<http://www.geology.gov.yk.ca/bedrock_terrane.html> [accessed May 15, 2013]; *also BC Geological Survey, GeoFile 2011-11*, .

Colpron, M., Nelson, J.L. and Murphy, D.C., 2006. A tectonostratigraphic framework for the pericratonic terranes of the northern Cordillera. *In:* Paleozoic Evolution and Metallogeny of Pericratonic Terranes at the Ancient Pacific Margin of North America, Canadian and Alaskan Cordillera, M. Colpron and J.L. Nelson (eds.), Geological Association of Canada, Special Paper 45, p. 1-23.

Colpron, M., Israel, S. and Friend, M., 2016a. Yukon plutonic suites. Yukon Geological Survey, Open File 2016-37, 1:750 000 scale.

Colpron, M., Israel, S., Murphy, D.C., Pigage, L.C. and Moynihan, D., 2016b. Yukon Bedrock Geology Map 2016. Yukon Geological Survey, Open File 2016-1, 1:1 000 000 scale.

Colpron, M., Murphy, D.C., Nelson, J.L., Roots, C.F., Gladwin, K., Gordey, S.P., Abbott, G. and Lipovsky, P.S., 2002. Preliminary geological map of Glenlyon (105L/1-7,11-14) and northeast Carmacks (115I/9,16) areas, Yukon Territory (1:125 000 scale). Exploration and Geological Services Division, Yukon Region, Indian and Northern Affairs Canada, Open File 2002-9; *also Geological Survey of Canada, Open File 1457*.

Cooper, G.R.J. and Cowan, D.R., 2011. A generalized derivative operator for potential field data. Geophysical Prospecting, vol. 59, p. 188-194.

Creaser, R.A., Heaman, L.M. and Erdmer, P., 1997. Timing of high-pressure metamorphism in the Yukon-Tanana terrane, Canadian Cordillera: constraints from U-Pb zircon dating of eclogite from the Teslin tectonic zone. Canadian Journal of Earth Sciences, vol. 34, p. 709-715.

Creaser, R.A., Goodwin-Bell, J.S. and Erdmer, P., 1999. Geochemical and Nd isotopic constraints for the origin of eclogite protoliths, northern Cordillera: implications for the Paleozoic tectonic evolution of the Yukon-Tanana terrane. Canadian Journal of Earth Sciences, vol. 36, p. 1697-1709.

de Keijzer, M., 2000. Tectonic evolution of the Teslin zone and the western Cassiar terrane, northern Canadian Cordillera. Unpublished PhD thesis, University of New Brunswick, Fredericton, NB, 391 p.

Erdmer, P., Ghent, E.D., Archibald, D.A. and Stout, M.Z., 1998. Paleozoic and Mesozoic high-pressure metamorphism at the margin of ancestral North America in central Yukon. Geological Society of America Bulletin, vol. 110, p. 615-629.

Gallagher, C., Brown, R.L. and Carr, S.D., 1998. Structural geometry of the Cassiar Platform and Teslin zone, Dycer Creek area, Yukon. *In:* Slave-Northern Cordillera Lithospheric Evolution (SNORCLE) Transect and Cordilleran Tectonic Workshop Meeting, F. Cook and P. Erdmer (eds.), Lithoprobe Report No. 64, p. 139-151.

Gallagher, C.S., 1999. Regional-scale transposition and late large-scale folding in the Teslin Zone, Pelly Mountains, Yukon. Unpublished MSc thesis, Carleton University, Ottawa, ON, 199 p.

Hansen, V.L., 1989. Structural and kinematic evolution of the Teslin suture zone, Yukon: Record of an ancient transpressional margin. Journal of Structural Geology, vol. 11, p. 717-733.

Hansen, V.L., 1992. *P-T* evolution of the Teslin suture zone and Cassiar tectonites, Yukon, Canada: Evidence for A- and B-type subduction. Journal of metamorphic Geology, vol. 10, p. 239-263.

Hansen, V.L., Mortensen, J.K. and Armstrong, R.L., 1989. U-Pb, Rb-Sr, and K-Ar isotopic constraints for ductile deformation and related metamorphism in the Teslin suture zone, Yukon-Tanana terrane, south-central Yukon. Canadian Journal of Earth Sciences, vol. 26, p. 2224-2235.

Hansen, V.L., Heizler, M.T. and Harrison, T.M., 1991. Mesozoic thermal evolution of the Yukon-Tanana composite terrane: new evidence from $^{40}Ar/^{39}Ar$ data. Tectonics, vol. 10, p. 51-76.

Harvey, J.L., Brown, R.L. and Carr, S.D., 1996. Progress in structural mapping in the Teslin suture zone, Big Salmon Range, central Yukon Territory. *In:* Slave-Northern Cordillera Lithospheric Evolution (SNORCLE) Transect and Cordilleran Tectonic Workshop Meeting, F. Cook and P. Erdmer (eds.), Lithoprobe Report No. 50, p. 33-44.

Harvey, J.L., Carr, S.D., Brown, R.L. and Gallagher, C., 1997. Deformation history and geochronology of plutonic rocks near the d'Abbadie fault, Big Salmon Range, Yukon. *In:* Slave-Northern Cordillera Lithospheric Evolution (SNORCLE) Transect and Cordilleran Tectonic Workshop Meeting, F. Cook and P. Erdmer (eds.), Lithoprobe Report No. 56, p. 103-114.

Hastie, A.R., Kerr, A.C., Pearce, J.A. and Mitchell, S.F., 2007. Classification of altered volcanic island arc rocks using immobile trace elements: Development of the Th–Co discrimination diagram. Journal of Petrology, vol. 48, p. 2341-2357.

Hayward, N. and Oneschuk, D., 2011. Geophysical Series, regional geophysical compilation project, Yukon Plateau, Yukon, parts of NTS 105, 106, 115 and 116. Geological Survey of Canada, Open File 6840, 1:750 000 scale.

Krogh, T.E., 1973. A low contamination method for hydrothermal decomposition of zircon and extraction of U and Pb for isotopic age determinations. Geochimica et Cosmochimica Acta, vol. 37, p. 485-494.

Krogh, T.E., 1982. Improved accuracy of U-Pb ages by the creation of more concordant systems using an air abrasion technique. Geochimica et Cosmochimica Acta, vol. 46, p. 637- 649.

Le Bas, M.J., Le Maitre, R.W., Streckeisen, A. and Zanettin, B., 1986. A chemical classification of volcanic rocks based on the total alkalis-silica diagram. Journal of Petrology, vol. 27, p. 745-750.

Levson, V., 1992. The sedimentology of Pleistocene deposits associated with placer gold bearing gravels in the Livingstone Creek area, Yukon Territory. *In:* Yukon Geology, Exploration and Geological Services Division, Yukon Region, Indian and Northern Affairs Canada, Volume 3, p. 99-132.

Mackie, R., Arne, D. and Pennimpede, C., 2016. Enhanced interpretation of stream sediment geochemical data for NTS 105E. Yukon Geological Survey, Open File 2016-9.

McLennan, S.M., 2001. Relationships between the trace element composition of sedimentary rocks and upper continental crust. Geochemistry, Geophysics, Geosystems, vol. 2, paper number 2000GC000109.

Mercier, M., 2011. Dextral strike-slip faulting history of the d'Abbadie fault zone, Pelly Mountains, south-central Yukon, Canada. Unpublished MSc thesis, Carleton University, Ottawa, ON, 148 p.

Mortensen, J.K., 1990. Geology and U-Pb geochronology of the Klondike District, west-central Yukon. Canadian Journal of Earth Sciences, vol. 27, p. 903-914.

Mortensen, J.K., 1992. Pre-Mid-Mesozoic tectonic evolution of the Yukon-Tanana terrane, Yukon and Alaska. Tectonics, vol. 11, p. 836-853.

Murphy, D.C., Mortensen, J.K., Piercey, S.J., Orchard, M.J. and Gehrels, G.E., 2006. Mid-Paleozoic to early Mesozoic tectonostratigraphic evolution of Yukon-Tanana and Slide Mountain terranes and affiliated overlap assemblages, Finlayson Lake massive sulphide district, southeastern Yukon. *In*: Paleozoic Evolution and Metallogeny of Pericratonic Terranes at the Ancient Pacific Margin of North America, Canadian and Alaskan Cordillera, M. Colpron and J.L. Nelson (eds.), Geological Association of Canada, Special Paper 45, p. 75-105.

Parrish, R.P. and Krogh, T.E., 1987. Synthesis and purification of ^{205}Pb for U-Pb geochronology. Chemical Geology, vol. 66, p. 103-110.

Pearce, J.A., 1982. Trace element characteristics of lavas from destructive plate boundaries. *In:* Andesites, R.S. Thorpe (ed.), John Wiley & Sons, p. 525-548.

Pearce, J.A., 1996. A user's guide to basalt discrimination diagrams. *In:* Trace element geochemistry of volcanic rocks: Applications for massive sulphide exploration, D.A. Wyman (ed.), Geological Association of Canada, Short Course Notes, Volume 12, p. 79-113.

Pearce, J.A. and Peate, D.W., 1995. Tectonic implications of the composition of volcanic arc magmas. Annual Reviews of Earth and Planetary Science, vol. 23, p. 251-285.

Pearce, J.A., Harris, N.B.W. and Tindle, A.G., 1984. Trace element discrimination diagrams for the tectonic interpretation of granitic rocks. Journal of Petrology, vol. 25, p. 956-983.

Petrie, M.B., Gilotti, J.A., McClelland, W.C., van Staal, C.R. and Isard, S.J., 2015. Geologic setting of eclogite-facies assemblages in the St. Cyr klippe, Yukon-Tanana terrane, Yukon, Canada. Geoscience Canada, vol. 42, p. 327-350.

Petrie, M.B., Massonne, H.-J., Gilotti, J.A., McClelland, W.C. and van Staal, C.R., 2016 *(in press)*. The P-T path of eclogite in the St. Cyr klippe, Yukon, Canada: Permian metamorphism of a coherent high-pressure unit in an accreted terrane of the North American Cordillera. European Journal of Mineralogy, vol. 28.

Piercey, S.J. and Colpron, M., 2009. Composition and provenance of the Snowcap assemblage, basement to the Yukon-Tanana terrane, northern Cordillera: Implications for Cordilleran crustal growth. Geosphere, vol. 5, p. 439-464, doi:10.1130/GES00505.1.

Piercey, S.J., Murphy, D.C., Mortensen, J.K. and Paradis, S., 2001. Boninitic magmatism in a continental margin setting, Yukon-Tanana terrane, southeastern Yukon, Canada. Geology, vol. 29, p. 731-734.

Piercey, S.J., Murphy, D.C., Mortensen, J.K. and Creaser, R.A., 2004. Mid-Paleozoic initiation of the northern Cordilleran marginal backarc basin: Geologic, geochemical, and neodymium isotope evidence from the oldest mafic magmatic rocks in the Yukon-Tanana terrane, Finlayson Lake district, southeast Yukon, Canada. Geological Society of America Bulletin, vol. 116, p. 1087-1106.

Piercey, S.J., Nelson, J.L., Colpron, M., Dusel-Bacon, C., Roots, C.F. and Simard, R.-L., 2006. Paleozoic magmatism and crustal recycling along the ancient Pacific margin of North America, northern Cordillera. *In:* Paleozoic Evolution and Metallogeny of Pericratonic Terranes at the Ancient Pacific Margin of North America, Canadian and Alaskan Cordillera, M. Colpron and J.L. Nelson (eds.), Geological Association of Canada, Special Paper 45, p. 281-322.

Proyer, A., 2003. The preservation of high-pressure rocks during exhumation: metagranites and metapelites. Lithos, vol. 70, p. 183-194.

Roddick, J.C., 1987. Generalized numerical error analysis with applications to geochronology and thermodynamics. Geochimica et Cosmochimica Acta, vol. 51, p. 2129-2135.

Roddick, J.C., Loveridge, W.D. and Parrish, R.R., 1987. Precise U/Pb dating of zircon at the sub-nanogram Pb level. Chemical Geology, vol. 66, p. 111-121.

Simard, R.-L., 2003. Geological map of southern Semenof Hills (part of NTS 105E/1,7,8), south-central Yukon (1:50 000 scale). Yukon Geological Survey, Open File 2003-12.

Simard, R.-L. and Devine, F., 2003. Preliminary geology of the southern Semenof Hills, central Yukon (105E/1,7,8). *In:* Yukon Exploration and Geology 2002, D.S. Emond and L.L. Lewis (eds.), Exploration and Geological Services Division, Yukon Region, Indian and Northern Affairs Canada, p. 213-222.

Simard, R.-L., Dostal, J. and Roots, C.F., 2003. Development of late Paleozoic volcanic arcs in the Canadian Cordillera: an example from the Klinkit Group, northern British Columbia and southern Yukon. Canadian Journal of Earth Sciences, vol. 40, p. 907-924.

Simard, R.-L., Dostal, J. and Colpron, M., 2007. Rifting of a Mississippian continental arc system: Little Salmon formation, Yukon-Tanana terrane, northern Canadian Cordillera. Canadian Journal of Earth Sciences, vol. 44, p. 1267-1289.

Stroink, L. and Friedrich, G., 1992. Gold-sulphide quartz veins in metamorphic rocks as a possible source for placer gold in the Livingstone Creek area, Yukon Territory, Canada. *In:* Yukon Geology, vol. 3, Yukon Geological Survey, p. 87-98.

Sun, S.S. and McDonough, W.F., 1989. Chemical and isotopic systematics of oceanic basalts: implications for mantle composition and processes. *In:* Magmatism in Ocean Basins, A.D. Saunders and M.J. Norry (eds.), Geological Society of London, Special Publication 42, p. 313-345.

Tempelman-Kluit, D.J., 1984. Geology, Laberge (105E) and Carmacks (105I), Yukon Territory. Geological Survey of Canada, Open File 1101, 1:250 000 scale.

Tempelman-Kluit, D.J., 2009. Geology of Carmacks and Laberge map areas, central Yukon: Incomplete draft manuscript on stratigraphy, structure and its early interpretation (*ca.* 1986). Geological Survey of Canada, Open File 5982, 399 p.

Westberg, E., 2009. Geological map of the 'Mendocina Creek' area (parts of 105E/8 and 105F/5). Yukon Geological Survey, Open File 2009-44, 1:50 000 scale.

Westberg, E., Colpron, M. and Gibson, H.D., 2009. Bedrock geology of western 'Mendocina Creek' (NTS 105F/5) and eastern Livingstone Creek (NTS 105E/8) areas, south-central Yukon. *In:* Yukon Exploration and Geology 2008, L.H. Weston, L.R. Blackburn and L.L. Lewis (eds.), Yukon Geological Survey, p. 227-239.

Winchester, J.A. and Floyd, P.A., 1977. Geochemical discrimination of different magma series and their differentiation products using immobile elements. Chemical Geology, vol. 20, p. 325-343.

Wood, D.A., 1980. The application of a Th-Hf-Ta diagram to problems of tectonomagmatic classification and to establishing the nature of crustal contamination of basaltic lavas of the British Tertiary volcanic province. Earth and Planetary Science Letters, vol. 50, p. 11-30.

Yardley, B.W.D., 1989. An introduction to metamorphic petrology. Longman Scientific & Technical, 248 p.

Yukon Geological Survey, 2016. Yukon Digital Bedrock Geology. Yukon Geological Survey, <http://www.geology.gov.yk.ca/update_yukon_bedrock_geology_map.html> [accessed November, 2016].

Yukon MINFILE, 2016. Yukon MINFILE – A database of mineral occurrences. Yukon Geological Survey, <ftp://ftp.geomaticsyukon.ca/GeoYukon/Geological/Mineral_Occurrences_250k/> [accessed November, 2016].

APPENDIX 1 (DIGITAL)

This appendix is only available digitally. It is available from http://data.geology.gov.yk.ca/.

Appendix 1. Additional GeoTIFFs and shapefiles derived from the geophysical data and produced to support interpretations discussed in text.

A) Residual total magnetic field data excluding the tie lines are gridded using the Geosoft™ bi-directional gridding algorithm with a cell size of 50 m, which is ¼ of the nominal line spacing. Azimuths of 160/340 and 020/200 are used for the bi-directional gridding. The resultant grids are rotated to the pole and the tilt derivatives calculated. Shading uses the generalized derivative operator of Cooper and Cowan (2011) with either a 160 or 020 direction (shown in Fig. 10; mag_res_50m_bi_70_RTP_TDR_withGenShading.tif)

B) Early conductivity data excluding the tie lines, based on the electromagnetic decays of channels 4 – 14 (0.018 – 0.103 ms) and calculated by Geotech (Boulanger *et al.*, 2016b; 2016a), are gridded using the Geosoft™ bi-directional gridding algorithm with a cell-size of 50 m, which is ¼ of the nominal line spacing. Azimuths of 160/340 and 020/200 are used for the bi-directional gridding (cond_early_50m_bi_70_TDR.tif).

C) North-northeast lineaments identified from magnetic intensity and conductivity data in Appendix 1a-b (NNE_mag_ln.shp; NNE_condEarly_ln.shp).

APPENDIX 2. ANALYTICAL METHODS FOR ISOTOPIC ANALYSIS PRESENTED IN TABLE 3.

Neodymium and hafnium isotopic data were collected on whole-rock powders at the Pacific Centre for Isotopic and Geochemical Research (PCIGR) at the University of British Columbia following the methods of Weis *et al.* (2005) with additional details provided in Piercey and Colpron (2009). Initial $^{143}Nd/^{144}Nd$ ratios and εNd were calculated at 360 Ma for the Mendocina and Last Peak greenstone, and 350 Ma for the Klinkit assemblage; the inferred age of these units is based on regional correlations. The chondritic uniform reservoir (CHUR) values used for εNd calculations are $^{143}Nd/^{144}Nd = 0.512638$ and $^{147}Sm/^{144}Nd = 0.1967$ (Hamilton et al., 1983). Depleted mantle model ages (T_{DM}) are calculated using the values of $^{143}Nd/^{144}Nd = 0.513163$ and $^{147}Sm/^{144}Nd = 0.2137$ (Goldstein *et al.*, 1984). Initial $^{176}Hf/^{177}Hf$ ratios and εHf were calculated at 360 Ma and 350 Ma, similar to the Nd isotopic data. The chondritic uniform reservoir (CHUR) values used for εHf calculations are $^{176}Hf/^{177}Hf = 0.282772$ and $^{176}Lu/^{177}Hf = 0.0332$ (Blichert-Toft and Albarede, 1997). Depleted mantle model ages (T_{DM}) are calculated using the values of $^{176}Hf/^{177}Hf = 0.28325$ and $^{176}Lu/^{177}Hf = 0.0334$ (Vervoort and Blichert-Toft, 1999). The results of Nd and Hf isotopic analyses are presented in Table 3.

REFERENCES

Blichert-Toft, J. and Albarede, F., 1997. The Lu-Hf isotope geochemistry of chondrites and the evolution of the mantle-crust system. Earth and Planetary Science Letters, vol. 148, p. 243-258.

Goldstein, S.L., O'Nions, R.K. and Hamilton, P.J., 1984. A Sm-Nd isotopic study of atmospheric dusts and particulates from major river systems. Earth and Planetary Science Letters, vol. 70, p. 221-237.

Hamilton, P.J., O'Nions, R.K., Bridgwater, D. and Nutman, A., 1983. Sm-Nd studies of Archaean metasediments and metavolcanics from West Greenland and their implications for the Earth's early history. Earth and Planetary Science Letters, vol. 63, p. 263-273.

Piercey, S.J. and Colpron, M., 2009. Composition and provenance of the Snowcap assemblage, basement to the Yukon-Tanana terrane, northern Cordillera: Implications for Cordilleran crustal growth. Geosphere, vol. 5, p. 439-464, doi:10.1130/GES00505.1.

Vervoort, J.D., Blichert-Toft, J., 1999. Evolution of the depleted mantle; Hf isotope evidence from juvenile rocks through time. Geochimica et Cosmochimica Acta, vol. 63, p. 533-556.

Weis, D., Kieffer, B., Maerschalk, C., Pretorius, W. and Barling, J., 2005. High-precision Pb-Sr-Nd-Hf isotopic characterization of USGS BHVO-1 and BHVO-2 reference materials. Geochemistry, Geophysics, Geosystems, vol. 6, 10 p., doi: 10.1029/2004GC000852.